Fluid Mechanics of Blood Clot Formation

Aaron L. Fogelson[1] and Keith B. Neeves[2]

[1]Departments of Mathematics and Bioengineering, University of Utah, Salt Lake City, Utah 84112; email: fogelson@math.utah.edu

[2]Department of Chemical and Biological Engineering, Colorado School of Mines, Golden, Colorado 80401

Annu. Rev. Fluid Mech. 2015. 47:377–403

First published online as a Review in Advance on September 18, 2014

The *Annual Review of Fluid Mechanics* is online at fluid.annualreviews.org

This article's doi:
10.1146/annurev-fluid-010814-014513

Keywords

platelets, coagulation, thrombosis, biotransport, biorheology

Abstract

Intravascular blood clots form in an environment in which hydrodynamic forces dominate and in which fluid-mediated transport is the primary means of moving material. The clotting system has evolved to exploit fluid dynamic mechanisms and to overcome fluid dynamic challenges to ensure that clots that preserve vascular integrity can form over the wide range of flow conditions found in the circulation. Fluid-mediated interactions between the many large deformable red blood cells and the few small rigid platelets lead to high platelet concentrations near vessel walls where platelets contribute to clotting. Receptor-ligand pairs with diverse kinetic and mechanical characteristics work synergistically to arrest rapidly flowing cells on an injured vessel. Variations in hydrodynamic stresses switch on and off the function of key clotting polymers. Protein transport to, from, and within a developing clot determines whether and how fast it grows. We review ongoing experimental and modeling research to understand these and related phenomena.

1. INTRODUCTION

Platelet: a small discoidal blood cell that plays a central role in clot formation

RBC: red blood cell

Endothelial cell (EC): a cell that lines blood vessels

Subendothelial (SE): pertaining to the extracellular matrix material and cells below the endothelial cell layer

Coagulation: a tightly regulated system of enzyme reactions that produces the enzyme thrombin

Platelet agonists: molecules, including collagen, ADP, and thrombin, that can trigger platelet activation

Fibrin: a protein produced from fibrinogen by thrombin that polymerizes into a fibrous gel

Thrombus: a clot in a blood vessel that is made of platelets, fibrin, and varying numbers of red and white blood cells from platelets and fibrin

Blood flows under pressure through the human vasculature. The pressure difference across the vascular wall means that a hole in the vessel wall can lead to rapid and extensive loss of blood. The hemostatic (blood clotting) system has evolved to seal a vascular injury quickly and minimize hemorrhage. The components of this system, so important to its ability to respond rapidly and robustly to overt injury, are implicated in the pathological processes of arterial and venous thrombosis that cause extensive death and morbidity.

Platelets are anuclear blood cells that have a discoid shape when circulating in their unactivated state. They have a diameter of approximately 2 μm, thickness of 0.5 μm, and a number density of 150,000–400,000 μl^{-1}. They are smaller and less numerous than the red blood cells (RBCs) that make up approximately 35–50% of the blood's volume, so individual platelets have a negligible effect on blood rheology (Turitto & Goldsmith 1996). Blood vessels are lined with endothelial cells (ECs). As the platelets circulate, they constantly monitor the integrity of the EC layer. If it is disrupted, then exposure of the blood to the subendothelial (SE) matrix and extravascular cells initiates the intertwined processes of platelet deposition and coagulation. When a platelet contacts the SE matrix, it adheres by bonds formed between receptors on the platelet's surface and molecules in the SE matrix (**Figure 1*a***). These bonds also trigger a suite of responses known as platelet activation, which includes the mobilization of additional families of binding receptors on the platelet's surface and the release of chemical agonists into the blood plasma. These agonists induce the activation of other platelets that do not directly contact the SE matrix. By means of molecular bonds that bridge the gap between newly mobilized binding receptors on two platelets' surfaces, platelets can cohere to one another. As a result of these processes, platelets deposit on the injured tissue, forming a platelet plug or aggregate (Jackson 2007, Ruggeri 2009).

Exposure of the SE matrix also triggers coagulation (**Figure 1*b***), which we view as consisting of two subprocesses. One involves a network of tightly regulated enzymatic reactions that begins with reactions on the damaged vessel wall and continues with reactions on the surfaces of activated platelets (Hoffman & Monroe 2001, Jesty & Nemerson 1995, Mann et al. 1990). The network's end product is the enzyme thrombin, which activates platelets and creates fibrin monomers that polymerize into a fibrous gel that stabilizes the clot. This polymerization process is the second subprocess of coagulation (Weisel 2005).

Many of these same processes occur when an atherosclerotic plaque ruptures in an artery and then produces a thrombus that quickly grows to occlude the vessel, thus triggering a heart attack. In venous thrombosis, thrombi consisting largely of fibrin and trapped RBCs, along with some platelets, can slowly grow to reach lengths of several centimeters. What initiates venous thrombosis is unclear but may involve a combination of sluggish flow behind venous valves and hypoxic or inflammatory stimulus of ECs that triggers coagulation and causes them to eject proteins that entrap platelets and leukocytes (Mackman 2012).

Platelet deposition and coagulation occur in the presence of moving blood and are strongly affected by fluid dynamics in ways that are only partially understood. One indication of flow's influence is that clots that form in veins, where blood flow is slow, are made mainly of fibrin gel (and trapped RBCs), whereas clots that form in arteries, where blood flow is fast, are made mainly of platelets. Elucidating the mechanisms by which fluid dynamics influences clot formation and stability is the aim of a growing level of experimental activity using, for example, microfluidic chambers, and of theoretical modeling and simulation using the tools of computational fluid dynamics. These studies, what has been learned from them, and what remains to be understood are the subjects of this review.

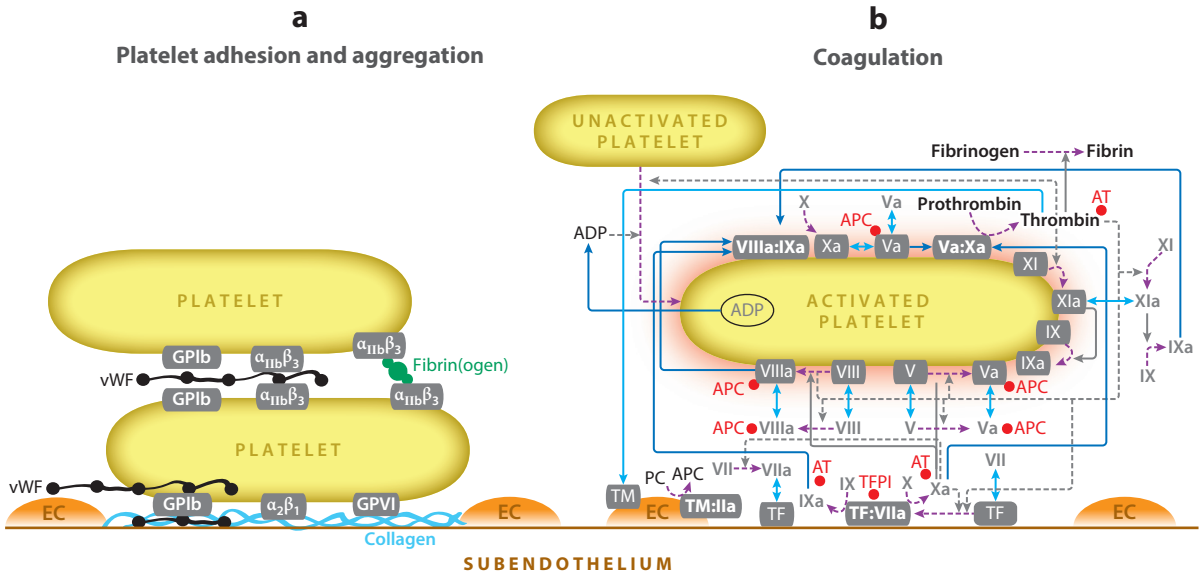

Figure 1

Platelet aggregation and coagulation schematics. (*a*) Platelet adhesion receptors and their ligands. Each platelet's surface bears ≈25,000 GPIb receptors that bind to surface-bound von Willebrand factor (vWF), ≈50,000 integrin $\alpha_{IIb}\beta_3$ receptors that bind to fibrinogen and vWF, ≈4,000 GPVI receptors and 1,000–4,000 integrin $\alpha_2\beta_1$ receptors that bind to several types of collagen. The integrins must be activated to form strong long-lived bonds. Collagen is a major constituent of the subendothelial (SE) matrix; fibrinogen is an abundant plasma protein; and vWF is adsorbed to SE collagen, circulates in plasma, and is secreted by endothelial cells (ECs). (*b*) Schematic illustration of coagulation reactions. Most coagulation proteins are named using Roman numerals [e.g., factor IX (FIX)] and exist in an inactive (FVIII) and active form (FVIIIa). FIIa (also known as thrombin), FVIIa, FIXa, FXa, and FXIa are enzymes; their inactive precursors are called zymogens. FVa and FVIIIa are cofactors for the enzymes FXa and FIXa, respectively, and must be activated from their precursors FV and FVIII. Tissue factor (TF) is a cofactor for FVIIa. The coagulation enzyme-cofactor complexes form on SE and platelet surfaces and have enzymatic efficiencies 10^5–10^6-fold those of the enzymes alone. The activation of a coagulation protein is by proteolysis (i.e., cutting) of the precursor by another enzyme. Thrombomodulin (TM) on ECs is a cofactor for thrombin in producing the inhibitor activated protein C (APC). Other major inhibitors are antithrombin (AT) and tissue factor pathway inhibitor (TFPI). Surface-bound enzyme complexes TF:VIIa, VIIIa:IXa, Va:Xa, and TM:IIa and other surface-bound species are shown in boxes. Also shown are cell or chemical activation (*purple lines*), movement in fluid or along a surface (*dark blue lines*), enzyme action in a forward direction (*solid gray lines*), the feedback action of enzymes (*dashed gray lines*), binding to or unbinding from surface (*light blue double-headed arrows*), and chemical inhibitors (*red circles*).

2. PLATELET MARGINATION IN FLOWING BLOOD

Blood is a dense suspension consisting of RBCs, leukocytes (white blood cells), and platelets in a protein-rich fluid called plasma. RBCs are biconcave with a long axis of ≈8.5 μm and are significantly more deformable than are the smaller ellipsoidal platelets and spherical leukocytes (≈10 μm). The rheology of blood is dominated by RBCs because they are by far the most numerous blood cells, with a volume fraction (also known as hematocrit) of 0.35–0.5 in humans. The extensive studies of blood's rheology are reviewed in Chien (1987) and Popel & Johnson (2005). Here, we focus on a process called margination by which platelets are concentrated near the vessel wall in flowing blood. Margination has an important physiological function in that platelets need to respond quickly to events on the vessel wall (e.g., injury). Leukocytes also marginate, but we discuss only platelets as they are the primary blood cell involved in clot formation.

Margination: the propensity of certain cells or particles to collect near the walls of a blood vessel under flow

2.1. Experimental Observations of Platelet Margination

von Willebrand factor (vWF): a large multimeric protein that plays a central role in platelet adhesion and aggregation, especially under high shear rates

Shear-induced diffusion (SID): apparent random motion of particles in flowing suspensions caused by collisions and other hydrodynamic interactions

In vivo observations show that flowing blood segregates into an RBC-rich core and an RBC-depleted near-wall region where platelets are concentrated. Intravital microscopy in the arterioles (d = 15–35 μm) of rabbits shows that platelet-sized spheres and platelets are concentrated in the RBC-depleted region at approximately twofold higher concentration than at the center line (Tangelder et al. 1982, 1985). Platelet concentrations near the wall are higher in arterioles than in venules, suggesting that higher shear rates lead to greater margination (Woldhuis et al. 1992).

Platelet margination enhances platelet accumulation at an injury site. Accumulation on collagen-rich SE matrix is 57-fold higher in whole blood than in a suspension of platelets alone and increases with increasing hematocrit (Turitto & Baumgartner 1975b, Turitto & Weiss 1980). Platelet adhesion to immobilized von Willebrand factor (vWF) also increases with hematocrit (0.2–0.6) for shear rates 1,000–10,000 s^{-1} (Chen et al. 2013).

The degree of margination of platelets and platelet-sized particles depends on the hematocrit and shear rate. Latex beads (2.4 μm) marginate at hematocrits of 0.15–0.45 and wall shear rates of >430 s^{-1} in 50- and 100-μm tubes (Tilles & Eckstein 1987). Platelets do not marginate at hematocrits of <0.10. There is fivefold higher concentration of beads in the 5–8-μm near-wall region compared to the core. The peak platelet concentration occurs a few micrometers off the wall (**Figure 2*a***). Platelet margination depends more strongly on the hematocrit than on the shear rate (Aarts et al. 1988, Zhao et al. 2007). A near-wall excess of platelets exists for steady and pulsatile flow in 3-mm tubes at a hematocrit of ≈0.5 (Xu & Wootton 2004).

Particles must exceed a certain size to marginate. Submicrometer particles marginate little in RBC suspensions at physiological shear rates, whereas 2–5-μm particles demonstrate significant margination (Charoenphol et al. 2010, Eckstein et al. 1988). Elliptical microparticles marginate more and are more likely to adhere to ECs than are spherical particles with equivalent diameters (Thompson et al. 2013). The enhanced adhesion of elliptical particles likely results from an increased contact area and reduced drag force compared to a sphere (Doshi et al. 2012, Watts et al. 2013).

Blood rheology and platelet margination are functions of RBC deformability. Experiments with fixed RBCs lead to reduced margination that is shear-rate independent (Eckstein et al. 1988). Increasing the viscosity of the suspending fluid from 1.2 to 3.9 cP, and thus increasing the stress on RBCs for a given shear rate, leads to platelet margination at lower shear rates (210 s^{-1}).

Figure 2

Red blood cell (RBC-)induced platelet margination and motion of platelets near wall-bound thrombi. (*a*) Plots of platelet lumenal position versus time during two-dimensional whole blood flow simulation showing margination in a 50-μm-wide channel at 1,100 s^{-1} and a hematocrit of 0.4. Panel *a* reproduced with permission from Crowl & Fogelson (2011). (*b*) Position-dependent mechanisms of platelet motion in flowing whole blood. Distance is measured from the vessel midline. (*c*) Snapshots in time of RBC and platelet positions and corresponding histograms of platelet lumenal location during a three-dimensional simulation of blood flow in a 34-μm channel at a shear rate of ≈1,000 s^{-1} and a hematocrit of 0.2. Distance from the bottom wall is measured in units of nominal RBC radius, 2.3 μm. Panel *c* adapted with permission from Zhao et al. (2012). (*d*) Sequence of snapshots of the movement of a platelet around a solid thrombus in a three-dimensional simulation of whole blood flow in a 7.5-μm-radius tube at a shear rate of ≈600 s^{-1} and a hematocrit of 0.1. Circles show evidence of RBC-induced platelet-thrombus interaction. Panel *d* adapted with permission from Wang et al. (2013a). (*e*) Superimposed snapshots (3 ms apart) of a platelet moving over a porous thrombus from a two-dimensional simulation of whole blood flow in a 50-μm-wide channel at a shear rate of 1,100 s^{-1} and a hematocrit of 0.4. (RBCs not shown.) Platelet motions from three different near-wall starting locations are shown. Panel *e* modified with permission from Skorczewski et al. (2013).

2.2. Models of Platelet Transport and Margination

The mechanism of platelet margination is still controversial, but several hydrodynamic forces are likely at play. The antimargination of RBCs in small vessels (10–500 μm), also called the Fåhræus-Lindqvist effect, leads to reduced hematocrit and apparent viscosity (Pries et al. 1992). The thickness of the RBC depletion layer is determined by a lift force that pushes RBCs away from

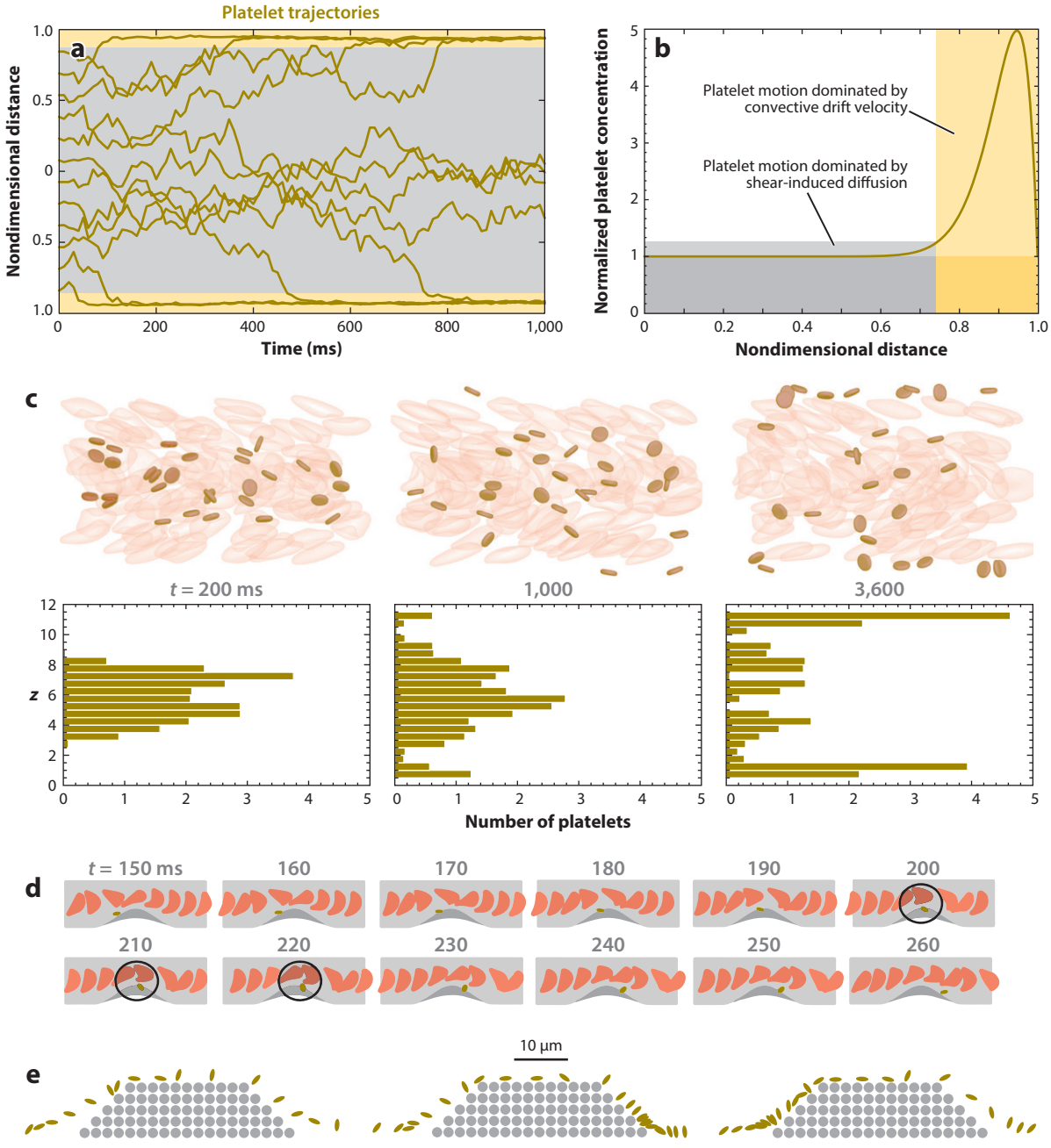

the wall, balanced by hydrodynamic collisions that push them toward the wall. A coarse-grained model of RBC hydrodynamics in a Couette flow suggests that the thickness δ of the depletion zone scales as $\delta \sim \mathrm{HCT}^{-1/2}$, where HCT is the hematocrit (Narsimhan et al. 2013). The lift force is caused by disturbances in the local velocity by the deforming, and thus asymmetrical, RBCs (Smart & Leighton 1991). Counteracting the lift force is shear-induced diffusion (SID), which describes the random motion of particles in a flowing suspension due to collisions with other particles (Eckstein et al. 1977, Leighton & Acrivos 1987, Phillips et al. 1992). The term collisions refers to flow-induced stresses and lubrication forces between particles and not rigid body collisions. The collisions are caused by gradients in particle density and suspending fluid viscosity that lead to the motion of particles in the flow direction and perpendicular to it.

Early experiments found that 2-μm tracer particles in RBC suspensions have a random-walk-like motion at low shear rates ($<30\ \mathrm{s}^{-1}$) (Goldsmith 1971). These observations suggest a diffusive flux model for lateral platelet transport:

$$J = -D_{\mathrm{eff}} \nabla \phi, \tag{1}$$

where J is the flux; D_{eff} the effective platelet diffusion coefficient; and ϕ the volume fraction of cells, which is essentially the hematocrit for whole blood. The diffusion coefficient of a platelet-sized particle estimated from the Stokes-Einstein equation is $O(10^{-9})\ \mathrm{cm}^2/\mathrm{s}$, whereas the platelet diffusivity estimated from solute transport models of platelet adhesion is $O(10^{-7})\ \mathrm{cm}^2/\mathrm{s}$ (Grabowski et al. 1972, Turitto et al. 1972). This indicates that Brownian motion can be neglected and that platelets' motion in flowing blood results from their interaction with RBCs or the perturbation of the suspending fluid by RBC motion.

A constant diffusion coefficient does not yield a net movement of platelets toward the wall and thus cannot explain their nonuniform distribution. Therefore, either a nonconstant diffusion coefficient or a bias must be added to explain these observations. Relationships from SID theory give nonconstant diffusion coefficients that are functions of the hematocrit and shear rate: $D_{\mathrm{eff}} = \gamma R^2 f(\phi)$, where γ is the shear rate, R is the particle radius, and $f(\phi)$ is a function of the particle volume fraction ϕ. For a suspension of rigid spheres, D_{eff} scales as ϕ^2 (Leighton & Acrivos 1987). For suspensions of deformable particles, including RBCs, maximal SID occurs at $\phi \sim 0.55$ (Zydney & Colton 1988) and decreases as ϕ approaches 1 owing to particle crowding. Alternatively, empirical power-law expressions have been derived for D_{eff} that are functions of the shear rate and hematocrit (Aarts et al. 1986, Turitto & Baumgartner 1975a).

A drift-diffusion model accounts for bias in platelet motion toward the wall (Eckstein & Belgacem 1991):

$$J = -vc - D_{\mathrm{eff}} \nabla c, \tag{2}$$

where $v = (0, 0, v_z)$ is the platelet drift velocity, and c is the platelet concentration. The spatially varying drift velocity was first estimated from experimental data (Yeh et al. 1994). Arguments based on the interaction of a platelet with a rotating RBC suggest that

$$v_z(z) = -\gamma R r \frac{d}{dz}\phi, \tag{3}$$

where R and r are the effective radii of an RBC and platelet, respectively, and z is the spatial coordinate in the direction perpendicular to the walls (Chen et al. 2013). The derivative of ϕ represents the RBC collision gradient, which is highest near the depletion layer. Using this expression in a stochastic differential form of a biased random walk gave platelet distributions in good agreement with experiments and direct lattice Boltzmann simulations.

2.3. Direct Cell Simulations of Platelet Margination

In the past decade, direct simulations of flowing blood cell suspensions have become possible. A recent review article provides details on simulation methods and challenges (Freund 2013). These simulations provide insight into the physical mechanisms that drive platelet margination at the cell scale.

A two-dimensional lattice Boltzmann immersed boundary method examined the contribution of the antimargination of RBCs, volume exclusion, and the timescales associated with the drift-diffusion process. Crowl & Fogelson (2011) considered pressure-driven flow in a 50-μm channel for shear rates of 400 and 1,100 s^{-1} and hematocrits of 0.2 and 0.4. In a simulation that would be virtually impossible in a laboratory experiment, they found that the timescale of platelet margination was independent of the initial RBC distribution (uniform versus antimarginated). This suggests that platelet margination is not caused by the antimargination of RBCs during the development of the RBC-depletion layer. However, the volume excluded by densely packed RBCs in the core does contribute to marginating platelets, although it does not give the experimentally measured dip in platelet concentration between the depletion layer and the vessel core. To estimate diffusion coefficients and the drift velocity, the authors compared results from direct cell simulations to those from simulations with a stochastic form of the flux in Equation 2. A novel finding was that a nonconstant diffusion coefficient was necessary to match the platelet fluctuations in the core. Diffusive motion is fastest at the midline and diminishes sharply as platelets approach the depletion layer. The drift mechanism is necessary to eject platelets into that layer (**Figure 2*b***) and to recover the platelet distribution over the timescale observed in direct cell simulations. The orientation and tank-treading motion of RBCs adjacent to the depletion layer may be the source of the drift mechanism.

A three-dimensional model of platelet margination using a Stokes flow boundary-integral method considered simple shear flow and channel flow in a 34-μm channel to investigate platelet margination (**Figure 2*c***) as a function of the RBC capillary number (Ca) (Zhao et al. 2012), defined as $\mathrm{Ca} = \mu\gamma R/E$, where μ is the plasma viscosity, γ the shear rate, R the RBC radius, and E the membrane shear modulus. In simple shear flow, platelet diffusion scales linearly with the shear rate for $\mathrm{Ca} > 1$ ($\gamma > 2{,}000\ s^{-1}$), as expected from SID theory. However, at lower Ca, there is a nonmonotonic dependence on the shear rate owing to increased fluctuations in RBC shape and orientation compared to the aligned, prolate ellipsoid RBC shape at high Ca. A similar dependence on Ca is found in channel flow, except there is a gradient in the hematocrit that yields a nonconstant diffusion coefficient in the core. There is a peak in the lateral platelet motion near the edge of the RBC depletion layer, in agreement with the findings of Crowl & Fogelson (2011). The diffusion coefficients estimated from three-dimensional simulations are an order of magnitude smaller than those from two-dimensional ones, but otherwise there is good agreement in the motion of platelet and tracer particles.

Another three-dimensional model used a lattice Boltzmann spectrin-link method to examine the effect of the hematocrit, the ratio between the internal RBC fluid to external fluid viscosity, and platelet size and shape in a 41-μm tube (Reasor et al. 2012). As in experiments, platelets marginated faster and to a greater extent with increasing hematocrit (0.2–0.4). Lower viscosity ratios led to enhanced margination owing to the faster tank-treading motion of the RBC membrane near the wall, and rigid RBCs gave no margination because they do not tank tread. Because of their flipping motion and ability to slide between RBCs, ellipsoids or disks marginated slower and to a lesser extent than did spheres. However, only spheres and ellipsoids interacted with the vessel wall, whereas disks tended to position themselves adjacent to RBCs at the edge of the depletion region.

ADP: adenosine diphosphate

Differences in deformability between platelets and RBCs also play a role in platelet margination. Kumar & Graham (2012) developed a model for binary suspensions of equal-sized particles with different deformabilities. In simulations at volume fractions of ≤ 0.2, they found that stiff particles marginate and floppy particles antimarginate if the stiff particles are dilute, as is the case for platelets in blood. This particle segregation primarily results from heterogeneous collisions between stiff and floppy particles.

A clot growing in the vessel lumen may alter the size of the depletion layer and the distribution of platelets within that layer. Modeling the thrombus as a porous structure predicts that the depletion layer narrows with increasing porosity (Skorczewski et al. 2013), thus squeezing platelets into the thrombus (**Figure 2*e***) and possibly increasing the likelihood of platelet aggregation. Even without interstitial fluid flow through a clot, the presence of a stenosis in a vessel (**Figure 2*d***) may enhance platelet deposition (Wang et al. 2013a).

3. SHEAR STRESS–DEPENDENT PLATELET ADHESION AND AGGREGATION

To carry out their role in hemostasis, platelets near the wall must adhere to the SE matrix exposed by injury. Platelets adhere primarily to collagen (types I, III, and VI) embedded in the SE matrix or to vWF molecules adsorbed to the collagen. The platelet surface bears numerous receptors that form bonds with these and other matrix proteins (**Figure 1*a***), and these bonds slow and then stop the platelet's motion on the vessel surface (Broos et al. 2011, Jackson 2007, Kasirer-Friede et al. 2014, Ruggeri 2009).

Platelet adhesion and aggregation occur over the full range of physiological shear rates (20–1,800 s^{-1}) and at much higher shear rates (up to 20,000 s^{-1}) that occur under pathological situations. At venous shear rates (<200 s^{-1}), bonds between glycoprotein VI (GPVI) receptors and collagen form and trigger the activation of integrin receptors ($\alpha_2\beta_1$ and $\alpha_{IIb}\beta_3$) sufficiently fast that the platelet is brought to rest and firmly adheres to the surface. Bonds between GPIb receptors and adsorbed vWF may play a role at these shear rates but are not essential. GPIb-vWF bonds become increasingly important at shear rates found in arteries (>500 s^{-1}) and arterioles (1,000–1,800 s^{-1}). Thus, a repertoire of receptors and surface-bound ligands, acting synergistically, is required to achieve adhesion over the range of flow conditions in the circulation. To varying but not fully characterized extents, the different platelet-surface bonds trigger intraplatelet signaling pathways that promote the platelet's activation response (Jackson et al. 2003, Savage et al. 1996).

Platelet activation consists of a number of diverse responses (Li et al. 2010). (*a*) The platelet's cytoskeleton reorganizes to extend pseudopodial appendages that help it spread out on the surface, become more firmly attached, and provide a lower profile that reduces drag force. (*b*) The platelet's $\alpha_2\beta_1$ and $\alpha_{IIb}\beta_3$ receptors become activated and mediate firm adhesion and spreading on the vascular surface. The $\alpha_{IIb}\beta_3$ receptors also enable platelet-platelet binding. (*c*) The lipid phosphatidylserine becomes exposed on the platelet surface, allowing it to support coagulation reactions. (*d*) The platelet secretes chemicals into the blood plasma. These chemicals provide a way to activate a platelet without its having to directly contact the injured vessel wall and allow the activation process to be propagated away from the wall (Andrews & Berndt 2004, Colman & Walsh 1987). Platelet activation is not an all-or-nothing process; some activation triggers cause only some of these responses to occur. There is significant evidence that different stimuli [e.g., collagen, adenosine diphosphate (ADP), thrombin] can act synergistically to promote a strong activation response (Chatterjee et al. 2010).

3.1. Adhesion at High Shear Stresses

Extensive studies have led to the picture that platelet adhesion at high shear stresses is a two-step process (Jackson 2007, Ruggeri 2009). First, transient bonds form between GPIb receptors and vWF. These bonds form rapidly, but also dissociate rapidly, and mediate a slow translocation of the platelet over the surface. Although often called rolling, it is unclear whether tumbling or sliding of the discoidal platelets is the dominant form of platelet motion along the surface. Second, the greatly retarded velocity of a rolling platelet compared to freely flowing platelets gives slower, but longer-lasting receptor-ligand bonds an opportunity to form and arrest the platelet's motion.

The local flow influences both bond formation and longevity and so strongly impacts which receptor-ligand bonds can mediate adhesion. For a platelet whose center is distance $\approx$1 μm from the vascular surface in a flow with shear rate γ, the maximum time τ that a receptor and ligand of characteristic size $\approx$10 nm will have to react is $\tau = O(10^{-2}/\gamma)$ s. In an arteriole with $\gamma \approx 1{,}000\ s^{-1}$, one obtains $\tau \approx 10^{-5}$ s. Only if the intrinsic binding rate k_{on} for a receptor-ligand pair is sufficiently high does it have a significant chance to bind. The longevity of a bond is impacted by the local flow as the dissociation rate k_{off} of a platelet-surface bond depends on the tensile force acting on the bond.

For many types of bonds, k_{off} is an increasing function of the force and thus, indirectly, of the local shear rate. Such a bond is called a slip bond. A catch bond is one for which k_{off} decreases when the force rises (Thomas et al. 2008). Yago et al. (2008) presented evidence that the GPIb-vWF bond has both catch and slip behavior (**Figure 3*b*,*c***). In force spectroscopy experiments of individual GPIb-VWF bonds, for applied forces below $\approx$20 pN, the bond lifetime increases with the force; for applied forces >20 pN, it decreases with force. The minimum $k_{off} = 3\ s^{-1}$ at 20 pN. In accord with these data, a platelet's rolling velocity on a vWF-coated surface decreases and becomes more uniform as shear stress increases up to a certain level and becomes faster and less stable for higher stress. Multiple studies suggest that GPIb-vWF bonds have fast association and dissociation rates, consistent with their ability to mediate transient adhesion of platelets under high-shear conditions (Arya et al. 2002b, Doggett et al. 2002, Yago et al. 2008). There is controversy about whether the GPIb-vWF bond is a catch bond and about its intrinsic kinetics (Kim et al. 2010, Miura et al. 2000).

The catch-bond behavior of the GPIb-vWF bond has important consequences. It can explain the observation of a shear threshold for vWF-mediated adhesion, that is, a minimum shear stress ($\approx$0.73 dyn/cm^2) below which platelet attachment does not occur (Doggett et al. 2002). These studies show platelets adhering by GPIb-vWF bonds at a shear stress of 3.0 dyn/cm^2, quickly dissociating when the shear stress was reduced to 0.3 dyn/cm^2 and adhering again when it was stepped back up to its original value. Furthermore, GPIb-vWF catch bonds between platelets flowing in the blood would have short lifetimes as the tensile force on such a bond is low. In contrast, GPIb-vWF catch-bond behavior may prolong platelet adhesion to a surface where larger forces are required. For a shear rate of 1,000 s^{-1}, Shankaran & Neelamegham (2004) estimated the force to attach a platelet to the surface to be 97 pN compared to 6 pN on a bond between flowing platelets. If several bonds share the attachment force, each will bear a low tensile force and have a high breaking rate. As some of the bonds break, the force on each remaining one will be higher, and their breaking rate will actually decrease. The data from Yago and others are useful for simulations of platelet adhesion and cohesion. Unfortunately, reliable information about the association rate of GPIb-vWF bonds is not available.

3.2. Aggregation in Two Steps

Aggregation refers to groups of platelets cohering to one another. For many years, it was assumed that platelets must be activated by soluble agonists before they can form cohesive bonds. This

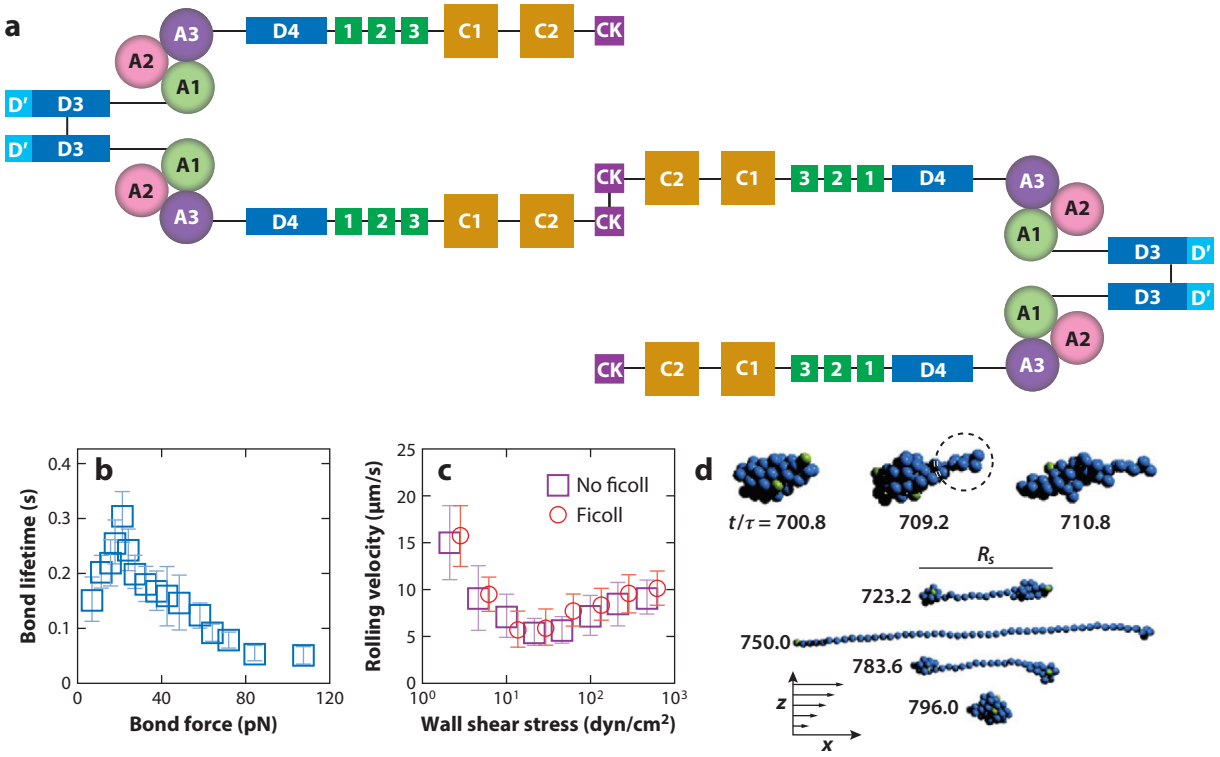

Figure 3

(*a*) Schematic illustration of a von Willebrand factor (vWF) multimer. The A1, A3, and C1 domains contain sites for binding to GPIb, collagen, and $\alpha_{IIb}\beta_3$, respectively; the A2 domain contains the cleavage site cut by ADAMTS-13. Panel *a* modified from Crawley et al. (2011). (*b*) Single-molecule-study measurements of the lifetime of a vWF-GPIb bond under force. (*c*) Velocity of the movement of a platelet on a vWF-coated surface as a function of shear stress. Panels *b* and *c* adapted with permission from Yago et al. (2008). (*d*) Images from a Brownian dynamics simulation of a vWF-like polymer extension and compaction cycle in a shear flow. The dashed circle denotes a thermally induced protrusion. The protruded part of the polymer is pulled by shear forces leading to nearly complete extension of the molecule. Subsequent rotation of the polymer results in shear-induced compaction. Panel *d* adapted with permission from Alexander-Katz et al. (2006).

mechanism is problematic, especially under fast flow, because it is unlikely that the soluble agonists would be found in the blood much upstream of a thrombus. Hence, the moving platelets would have to be activated very quickly by agonists in the immediate vicinity of the thrombus.

There is growing acceptance of the idea that the deposition of additional layers of platelets, like that of the first layer on the vessel surface, is a two-step process that involves vWF that is immobilized on the lumenal surface of adherent platelets through bonds with $\alpha_{IIb}\beta_3$ (Jackson 2007, Ruggeri 2009). To begin, unactivated platelets transiently bind to the thrombus using their GPIb receptors to attach to these immobilized vWF molecules. This slows the platelets and allows time for soluble agonists or signals triggered by the GPIb-vWF bonds to activate them, enabling longer-lived and strong $\alpha_{IIb}\beta_3$-mediated bonds to form (Jackson 2007, Ruggeri et al. 1999, Savage et al. 1998).

A platelet in a thrombus has to support the increasing detachment force on it as platelets accumulate on top of it, forming a structure that projects well into the vessel. To do this, many long-lived bonds are required. The bond between $\alpha_{IIb}\beta_3$ (in its high-affinity state) and fibrinogen

has off rates of 0.15–0.25 s^{-1} for applied forces up to 50 pN and a most-probable breaking force of 90 pN (Litvinov et al. 2011, 2012). These off rates are much smaller than those for GPIb-vWF, consistent with the $\alpha_{IIb}\beta_3$ fibrinogen bond's ability to mediate firm platelet adhesion to a surface and firm cohesion between platelets, even under high-shear forces. The $\alpha_{IIb}\beta_3$ receptor can also bind with vWF, but no binding rate data are available for these bonds.

The current picture of platelet aggregation under flow is that both fibrinogen and vWF play a role at all physiological shear rates (Neeves et al. 2013, Ruggeri et al. 1999, Savage et al. 1998), with vWF becoming essential at higher shear rates. In experiments at high shear rates (1,500–1,800 s^{-1}) without fibrinogen, aggregates form rapidly but are unstable, and by shedding individual platelets or small groups of them, the aggregates disintegrate, leaving only a monolayer of adherent platelets. In contrast, with both vWF and fibrinogen, the aggregates grow more slowly, but they are stable and remain intact for extended periods of time. Matsui et al. (2002) tracked the spatial and temporal distributions of fluorescently labeled vWF and fibrinogen within aggregates growing on a collagen-coated surface at a shear rate of 1,500 s^{-1}. They found that vWF was always required to attach platelets to parts of the aggregate exposed to fast flow. In the interior of the aggregate, in which the flow was presumably much slower, fibrinogen gradually replaced vWF as the molecule mediating interplatelet cohesion. These experiments show that the interactions and participation of different components of the system are orchestrated both in time and in space, at least partly in response to differences in the local flow environment.

Almost all aggregation experiments have been done with anticoagulated blood, so that no thrombin or fibrin would be produced, in order to isolate platelet-surface and platelet-platelet interactions. But thrombin and fibrin produced during coagulation can influence platelet accumulation by activating additional platelets and stabilizing platelet thrombi, so one cannot extrapolate the results of these experiments directly to situations in which coagulation is also occurring, such as in vivo. Recently, some experimental work looking at platelet aggregation and coagulation under flow has been reported (Colace et al. 2012, Okorie et al. 2008, Onasoga-Jarvis et al. 2014), and it has provided extremely valuable data to validate and inform mathematical modeling of the type described in Section 5.

3.3. Aggregation Modeling

Mathematical modeling and computer simulation of clotting are essential in our efforts to understand how the clotting system as a whole, or even major pieces of it, functions as an integrated dynamical system. Yet modeling of platelet adhesion and aggregation, coagulation, and fibrin polymerization presents enormous challenges both in formulating models and in studying them computationally. To look at thrombus development beyond initial adhesion, one must account for the disturbance to the flow that the growing thrombus engenders. Hence, models of thrombus growth involve, at a minimum, a coupled problem of fluid dynamics, transport of cells and chemicals, platelet activation, adhesion and cohesion mechanics, and growth of a fluid-perturbing platelet mass. These processes involve spatial scales ranging from millimeters to nanometers and timescales from minutes to milliseconds. The interactions themselves are diverse, making clotting a prime example of a multiphysics problem.

The first models that accounted for the mutual interaction of fluid dynamics and platelet aggregation were Fogelson's discrete aggregation models (Fogelson 1984, Fogelson & Guy 2008, Fogelson et al. 2003) and continuum aggregation models (Fogelson 1992, 1993; Fogelson & Guy 2004; Wang & Fogelson 1999) aimed at events in small arterioles and larger arteries, respectively. In the past decade, there has been an upsurge in efforts to model important aspects of the clotting system that involve fluid dynamics, aided by increases in computing power, the development of

new computational methods for fluid-structure interaction problems, a wealth of new data about bond dynamics and mechanics, and greatly improved capacity to do in vitro experiments of clotting under flow (Colace et al. 2012, Mizuno et al. 2008, Okorie et al. 2008, Onasoga-Jarvis et al. 2013) and to observe it in vivo (Furie & Furie 2005, Welsh et al. 2012). Most models track the motion and interactions of discrete elements representing the platelets and so describe events in small vessels or microfluidic devices. The platelet-fluid interaction problem has been tackled using a range of approaches, including the immersed boundary method (Fogelson & Guy 2008), the force-coupling method (Pivkin et al. 2006), a variety of particle methods (Filipovic et al. 2008; Kamada et al. 2010, 2013; Mori et al. 2008; Pivkin et al. 2009; Tosenberger et al. 2013), the cellular Potts model (Xu et al. 2008, 2009, 2010), and a hybrid lattice kinetic Monte Carlo–lattice Boltzmann method (Flamm et al. 2011). Related research has looked in detail at interactions between pairs of platelets using boundary-integral methods (Mody & King 2008a,b; Wang et al. 2013b). These models all treat cell-cell binding, whether by using attractive potentials between particles (e.g., Pivkin et al. 2006), prescribing rules for cell binding and unbinding (Flamm et al. 2011), using coarse-grained elastic links between platelets to represent ensembles of bond types (Skorczewski et al. 2014), or incorporating detailed Monte Carlo treatments of formation and breaking of individual vWF-GPIb bonds (Mody & King 2008b, Wang et al. 2013b). The work in Xu et al. (2010) and Flamm et al. (2011) includes treatments of the coagulation reactions and intraplatelet signaling, respectively.

Continuum models treat platelets in terms of their number densities. Those in Fogelson (1992) and Fogelson & Guy (2004, 2008) treat macroscale platelet thrombosis in atherosclerotic arteries and track the stresses developed by interplatelet bonds using an Oldroyd-B-like evolution equation. Those in Leiderman & Fogelson (2011, 2013) look at interactions among platelets and coagulation biochemistry, treating the growing thrombus as a porous medium whose porosity depends on the number density of bound platelets. **Figure 4** shows results from several of the aggregation models; the platelet-coagulation models are discussed further below. Three recent reviews provide more details of these models (Flamm & Diamond 2012, Wang & King 2012, Xu et al. 2011).

4. FORCE-DEPENDENT FUNCTION AND REGULATION OF VON WILLEBRAND FACTOR

vWF is a soluble protein that is at the center of the story of platelet adhesion and aggregation because of its unique ability to initiate these processes under high-shear conditions. Here, we focus

Figure 4

Simulations of platelet aggregation. (*a*) Sequence of temporal snapshots from a three-dimensional immersed boundary simulation of platelet aggregation onto a collagen-coated surface. Balls are platelets (their colors have no meaning), light blue line segments represent platelet-wall and platelet-platelet bonds, and the wavy red surface is the adenosine diphosphate (ADP) threshold concentration isosurface. Panel *a* reproduced with permission from Fogelson & Guy (2008), originally adapted from Fogelson et al. (2003). (*b*) Snapshots from simulations of thrombosis following a stenotic plaque rupture using the platelet aggregation continuum model. (*Left column*) Rupture at an upstream high-shear region. (*Top*) Aggregate bond density (*red*) and an above-threshold activation chemical (*gray*) showing the embolization of platelet masses in response to a large strain. (*Bottom*) Strain in aggregates is high (*dark red*) where the shear stress is high and is low (*green*) where the shear stress is low. (*Right column*) Rupture at a downstream low-shear region. (*Top*) Aggregate growing slowly and stably, largely sheltered by the plaque. (*Bottom*) High strain is limited to the top edge of the aggregate where local shape remodeling but not embolization occurs. Panel *b* adapted with permission from Fogelson & Guy (2008), based on the model in Fogelson & Guy (2004). (*c*) Snapshot in time of lattice kinetic Monte Carlo simulation of platelet aggregation showing flow streamlines, ADP concentration field (*orange* for high and *blue* for low), and platelets in different activation states (*black circles* are unactivated, and *white circles* are fully activated). Note the localized pockets of high ADP concentration. Panel *c* reproduced with permission from Flamm et al. (2012). (*d*) Snapshot in time from platelet thrombosis simulation using the cellular Potts model. Colors show cells in different states of activation. Flow is left to right in each simulation. Panel *d* reproduced with permission from Xu et al. (2008).

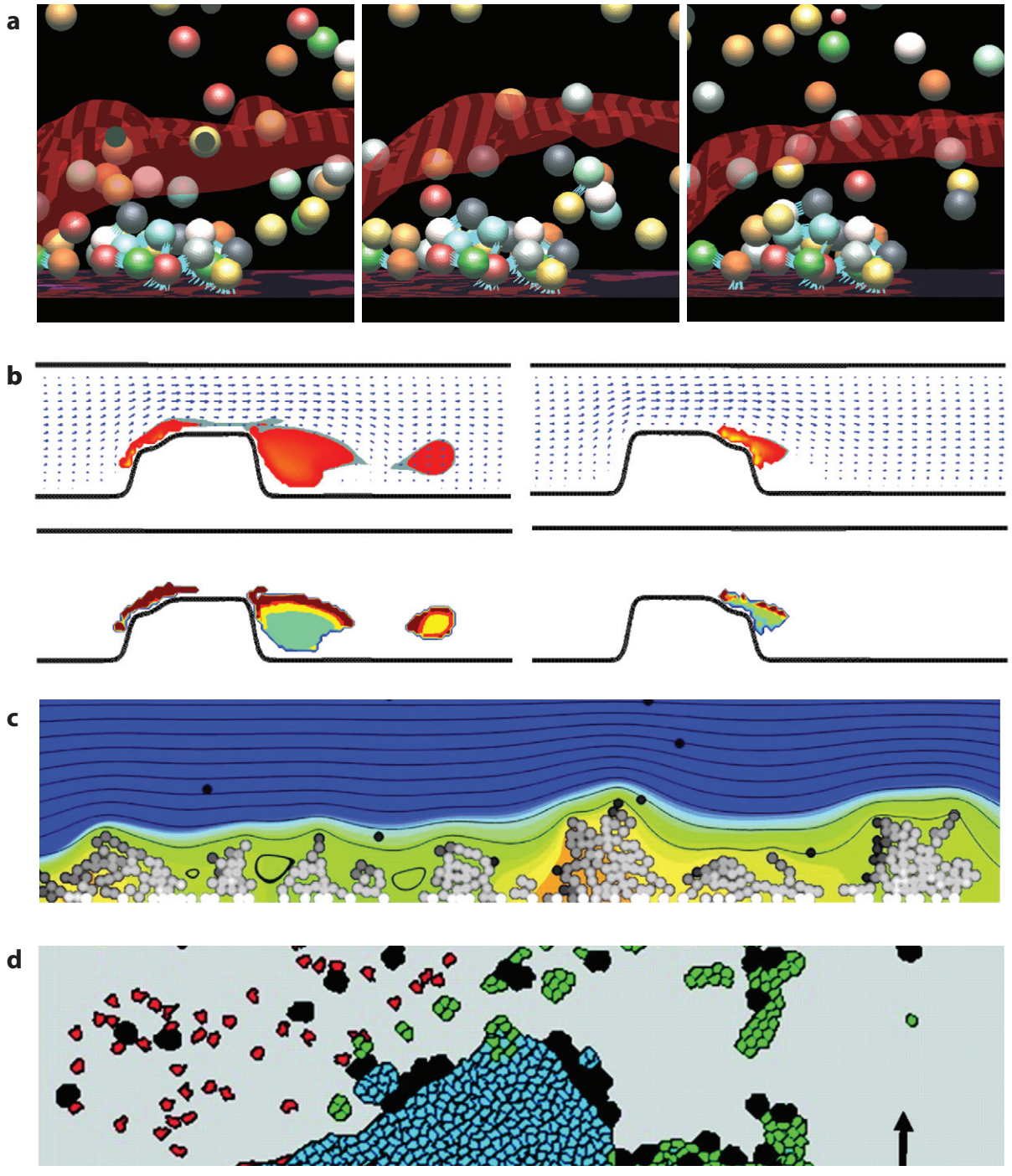

on vWF because fluid dynamic forces are of fundamental importance to its function and regulation. Circulating vWF multimers are linear chains with varying numbers of identical dimeric subunits. Thrombotic pathologies arise if the circulating multimers are too long, and bleeding occurs if they are too short (Zhou et al. 2010). Clearly, the proper function of the hemostatic system requires plasma vWF multimers to fall within a range of lengths. This prompts two questions: What is it about the length of the vWF multimer that makes it important that it fall within a certain range? How does the body normally keep the lengths within this range? It is now clear that the answers to both questions depend on the behavior of the multimers under different flow and hydrodynamic force regimes. To explain this, we need some background about vWF and about the enzyme ADAMTS-13, which can cut a long multimer into shorter ones.

4.1. von Willebrand Factor Conformation Under Stress

vWF monomers join head-to-head to form a dimer; dimers join tail-to-tail to form a multimer (**Figure 3*a***). Each monomer has a sequence of protein domains; the most important for us are the consecutive A1-A2-A3 domains and the nearby C1 domain. The A1, C1, and A3 domains contain binding sites for the GPIb and activated $\alpha_{IIb}\beta_3$ receptors and collagen, respectively. The A2 domain contains the site that can be cut by ADAMTS-13 (Crawley et al. 2011). Each subunit has a length of approximately 70 nm, and the multimers that normally circulate have fully extended lengths of 1–2 μm; hence they consist of 15–30 subunits.

vWF is produced by ECs and is also stored in the α-granules of platelets. Platelet vWF consists of long multimers that are secreted by an activated platelet. ECs secrete vWF continually at a basal level, mostly as individual moderate-length multimers; lumenally into the blood; and ablumenally into the SE matrix (Dong 2005). The bulk of EC vWF is packaged as long chains in a structure called a Weibel-Palade body. When an EC is activated by coagulation proteins, inflammatory signals, or shear stress, vWF is expelled from its Weibel-Palade bodies into the blood (Galbusera et al. 1997, Turner et al. 2009). It rapidly unfurls into ultralarge vWF (UL-vWF) multimers that can anchor to ECs and extend downstream along the vascular wall. UL-vWF can reach lengths of hundreds of micrometers, implying that it may have thousands of subunits. UL-vWF is hyperactive in terms of its binding to platelets and collagen (Moake et al. 1986, Turner et al. 2012) because it has many A1 and A3 binding sites and because the individual bonds between GPIb receptors and UL-vWF A1 domains are stronger than those for the moderate-length multimers normally found in the plasma (Arya et al. 2002a). Unlike normal plasma multimers, UL-vWF multimers can spontaneously bind to GPIb receptors at shear stresses encountered in a healthy circulation. Although UL-vWF multimers are helpful at the site of a vascular injury, they cannot circulate without causing severe problems. An example is the fatal condition thrombotic thrombocytopenic purpura in which platelet thrombi form throughout the microvasculature as a result of serious deficiency of the ADAMTS-13 enzyme, which regulates vWF size (Zhou et al. 2010).

vWF circulates in a compact globular conformation, but to interact with platelets, it must be in an extended conformation. To study this issue, Schneider et al. (2007) performed microfluidic studies under controlled shear and directly observed the dynamics of a vWF molecule free in solution. They found that below a critical shear stress, the multimer had a collapsed globular conformation with a diameter of approximately 2 μm. When the shear stress was increased to ≈50 dyn/cm^2, the multimer suddenly elongated to approximately 15 μm and then displayed cycles of extension and compaction between the globular and elongated conformations. It returned quickly to its globular conformation when flow was stopped. Performing additional studies in the presence of a collagen-coated surface, the authors saw little vWF deposition until, at a critical shear stress with a magnitude similar to that for extension, deposition suddenly increased substantially. They

attributed this increase in deposition to the exposure of many vWF A3 domains on the extended molecules, which in turn allowed the simultaneous binding of each multimer to collagen at multiple locations.

vWF's sudden elongation at high shear is very different from the gradual elongation of other polymers (e.g., DNA) at much lower shear stresses. Brownian dynamics simulations show that, to reproduce the sudden elongation at high shear rates, simulations had to include hydrodynamic effects, the monomers had to be large (≈50–100 nm; as they are for vWF), and nonspecific attractive forces between monomers had to be sufficiently strong but not too strong (e.g., $1–2k_BT$) (Alexander-Katz & Netz 2008, Alexander-Katz et al. 2006, Schneider et al. 2007). The simulations suggest a mechanism initiated when thermal motion causes polymer segments to protrude from the globular surface. If the drag force on the protrusion exceeds the restoring force from the attraction between monomers, then the protrusion nucleates an elongation cycle (**Figure 3*d***). Because the polymer tumbles in the shear flow, it later is subject to compressive fluid forces and returns to its globular shape until another elongation cycle begins. Scaling arguments show that the critical shear stress for elongation depends strongly on the monomer size and less strongly on the overall polymer length. The authors argue that the large size of the vWF monomer is essential for plasma vWF to generally be in a globular conformation in which it does not cause spontaneous platelet aggregation. Additional simulations of elongational flows (Sing & Alexander-Katz 2010, 2011) showed an even-sharper transition in the polymer's length at a critical elongation rate. This may come into play in elongational flows accompanying vessel transection or in a damaged vessel undergoing vasoconstriction.

4.2. Regulation of von Willebrand Factor Multimer Size

For a healthy person, circulating vWF multimers are of moderate, but varying size. Because the enzyme ADAMTS-13 is constitutively active and has no known inhibitors in plasma, the question arises as to why plasma vWF multimers are not reduced to a uniform minimum size. The answer seems to be that ADAMTS-13's access to the cleavage sites on vWF is mechanically regulated by fluid stresses.

In its globular conformation, vWF's A1 and A2 domains are hidden inside the folded molecule, but at least some of its A3 domains are exposed (Crawley et al. 2011). Globular vWF cannot bind to platelets or be cleaved by ADAMTS-13, but it can bind to SE collagen if it becomes exposed to the blood. When vWF is in an extended conformation, many of its A1, A2, and A3 domains are accessible, and they provide a periodic string of reactive sites for binding to platelets and collagen and cleavage sites for ADAMTS-13. This dynamic is interesting because when platelets bind to the elongated vWF, increased tensile forces occur that further stretch the multimer, unfold more of its A2 domains, and potentially lead to a reduction in the multimer's size.

Single-molecule studies of A2 domain unfolding, using isolated A2 domains (Zhang et al. 2009), A1-A2-A3 tridomain constructs (Wu et al. 2010), or actual vWF multimers (Ying et al. 2010), indicate that the A2 domain must unfold prior to its cleavage by ADAMTS-13. The forces required to unfold the A2 domain are larger when it is flanked by the A1 and A3 domains than when it is isolated. Theoretical estimates suggest that tensile forces of the requisite size may arise in the centers of extended large multimers, but not for smaller multimers (Zhang et al. 2009). This provides a mechanism for preventing cleavage of multimers of less than a certain length.

When UL-vWF is released from an EC, anchors to the cell, and stretches downstream, its A2 domains are unfolded, and again the stretching is enhanced when platelets are bound to the multimer. ADAMTS-13 is known to bind to some of the exposed A2 domains and cleave them. Several studies have shown that the sizes of multimers released from the EC surface after cleavage

by ADAMTS-13 are still much longer than typical plasma vWF multimers (De Ceunynck et al. 2011, Jin et al. 2009), suggesting that further size regulation occurs elsewhere. In vitro studies of vWF cleavage show that vWF bound to multiple platelets in shear flow (and thus subject to much higher tensile force than are free vWF molecules) is a preferred substrate for ADAMTS-13 (Shim et al. 2008). The extent that ADAMTS-13 regulates thrombus growth by cleaving vWF within a growing thrombus is a subject of current research (Chauhan et al. 2006).

Shear-induced platelet aggregation (SIPA): aggregation of platelets in flowing blood induced by unusually high shear stress

4.3. von Willebrand Factor and Aggregation Under Pathological Shear

vWF plays an essential role in shear-induced platelet aggregation (SIPA). In in vitro experiments, platelets, subject to pathologically high shear rates ($>5{,}000\ s^{-1}$) for $\approx$1 min, aggregate without contact with surfaces or application of exogenous activators (Moake et al. 1986). SIPA is associated with cardiovascular disease. For example, SIPA and platelet binding to vWF are enhanced in plasma from patients with recent heart attacks compared to normal plasma, and the level of vWF in these patients indicates their likelihood of future heart attacks (Spiel et al. 2008). Larger vWF multimers normally found in the plasma contribute to this process, and both platelet GPIb and $\alpha_{IIb}\beta_3$ receptors are involved (Goto et al. 1995, Moake et al. 1986, Peterson et al. 1987). SIPA also involves the platelet release of ADP (Moake et al. 1988), probably to reinforce the activation of the releasing platelet itself or of its immediate neighbors, as ADP would be rapidly dispersed in high-shear flows. It is presumed that SIPA involves the stress-mediated extension of vWF multimers and that high tensile forces on the GPIb-vWF bonds trigger this initial platelet activation, but this has not been directly established. vWF self-association may also contribute. This involves the transient binding under high shear of multimers into long strings or thick fibers. It occurs with plasma vWF becoming associated with collagen-bound vWF (Colace & Diamond 2013, Savage et al. 2002), on platelet GPIb receptors (Dayananda et al. 2010), and in the plasma (Shankaran et al. 2003). By increasing the effective size of the molecule bound to GPIb, the tensile force on the receptor and the possibility of mechanically triggered platelet activation increase.

Experiments at even higher shear rates ($10{,}000–30{,}000\ s^{-1}$) reveal other vWF-dependent aggregation processes in which platelets do not have to be activated in order to cluster in large groups for extended periods of time (Ruggeri et al. 2006) and in some of which rapid changes in geometric features and shear stresses seem to be involved (Jackson et al. 2009, Maxwell et al. 2007, Westein et al. 2013).

5. MASS TRANSFER LIMITATIONS OF CLOT GROWTH

The coagulation reactions are initiated when injury exposes the cell-bound protein tissue factor (TF) to the blood (**Figure 1*b***). The first coagulation enzymes are produced on the SE matrix and are released into the flowing blood. Some of these enzyme molecules bind to activated platelets adhered to the SE matrix and participate in the formation of a sequence of enzyme complexes that propagate the pathway to thrombin production. Thrombin produced on the platelet surface feeds back on the enzyme network to accelerate its own production, activates additional platelets, and converts soluble fibrinogen molecules in the plasma into insoluble fibrin monomers. The fibrin monomers polymerize into protofibrils, and these laterally aggregate into thicker fibers. A branching network of fibers grows between and around the platelets in a wall-bound platelet aggregate. Coagulation is kinetically limited by anticoagulation pathways but is also regulated by mass transfer limitations connected with the transport of the zymogens to and enzymes away from the injury site. Experimental and computational studies have shown that these mass transfer limitations are biophysical mechanisms that regulate clot growth.

5.1. Mass Transfer Regulation of Surface Coagulation Reactions and Fibrin Polymerization

Three enzyme complexes assemble on the subendothelium and activated platelet surfaces and are regulated in part by mass transfer limitations. SE-bound TF:FVIIa initiates coagulation by converting zymogens FX and FIX to FXa and FIXa. FIXa binds to FVIIIa on the surface of an activated platelet to form the FIXa:FVIIIa (tenase) complex, which produces more FXa. Similarly, platelet-bound FXa and FVa bind together to form the FXa:FVa complex (also known as prothrombinase) that catalyzes the conversion of prothrombin to thrombin. Blood flow can either promote or inhibit these surface reactions, depending on the shear rate. FXa production by TF:FVIIa is transport limited at shear rates of $<600\ s^{-1}$ (i.e., the FXa flux increases with increasing shear rate) (Gemmell et al. 1990). In contrast, FXa production is reaction limited (its flux is constant) for shear rates of $>600\ s^{-1}$. When both TF:FVIIa and FVIIIa:FIXa are present, their combined FXa production is transport limited from $57\ s^{-1}$ to $1{,}130\ s^{-1}$ (Repke et al. 1990). Thus, blood flow enhances the initiation of coagulation for all physiological shear rates, provided that normal concentrations of FVIII, FIX, and FX are present. Thrombin production by prothrombinase in a phospholipid bilayer is reaction limited for shear rates of 100–1,000 s^{-1} (Haynes et al. 2011). Flow acts as an inhibitor by diluting thrombin and thus localizing high thrombin concentrations to the immediate vicinity of a clot.

Regardless of the shear rate, a threshold TF surface density is necessary to initiate coagulation. This threshold behavior was first predicted by simulations of clot formation on immobilized TF (Kuharsky & Fogelson 2001) and was confirmed by in vitro blood flow assays over 175-μm spots containing TF and collagen (Okorie et al. 2008). The threshold TF density required to initiate coagulation under flow increases threefold as the shear rate increases from 100 to 1,000 s^{-1}. A certain injury size is also necessary to initiate coagulation both statically and under flow on immobilized TF in lipid bilayers (Kastrup et al. 2007, Shen et al. 2008). Presumably vessel walls are always subject to some degree of disruption and thus TF exposure. The thresholds likely ensure that coagulation is initiated only on injuries that are sufficiently large or deep to expose high densities of TF.

Fibrin polymerization can be either transport or reaction limited, depending on the thrombin wall flux and shear rate (Neeves et al. 2010). A kinetic model of fibrin gel formation predicts two regimes of growth depending on the shear rate and gel permeability (Guy et al. 2007). At low shear rates, growth is limited by the transport of thrombin from the procoagulant surface to the surface of the gel. The rate of thrombin transport is determined by the hydraulic permeability, which varies over three orders of magnitude for fiber volume fractions of 0.02–0.54 (Wufsus et al. 2013). At high shear rates, growth is limited by the dilution of fibrin polymers before they can reach a gelation concentration. This agrees with experiments in purified systems that show little or no fibrin gelation at a wall shear rate of $100\ s^{-1}$ on flat substrates, even at high thrombin concentrations (1 μM) (Neeves et al. 2010). Surfaces with a micrometer-scale roughness provide some protection of polymerization products from dilution by flow. For example, 800-nm TF-coated beads support the initiation of fibrin formation at $1{,}000\ s^{-1}$ (**Figure 5*a***) at a sufficiently high TF surface density (Onasoga-Jarvis et al. 2014), but the gel's ultimate growth into a channel is limited to 10–15 μm at $100\ s^{-1}$, which is similar to predicted gel heights in computational models (Guy et al. 2007).

The large burst of thrombin that follows the initiation of coagulation results in platelet activation and the aggregation and polymerization of fibrin. It is important that these events be localized to the injured region so as not to cause systemic clotting. There are endogenous biochemical pathways that inhibit coagulation, including antithrombin and the activated protein C (APC) pathway.

Antithrombin is distributed throughout the plasma, but APC is produced on ECs by a complex formed when thrombin binds to EC-bound thrombomodulin. Because the EC surface on which this occurs is likely downstream of the injury, it is questionable whether the APC can affect the local clot growth (Fogelson & Tania 2005). It more likely functions to scavenge active coagulation molecules that flow has carried away from the clot.

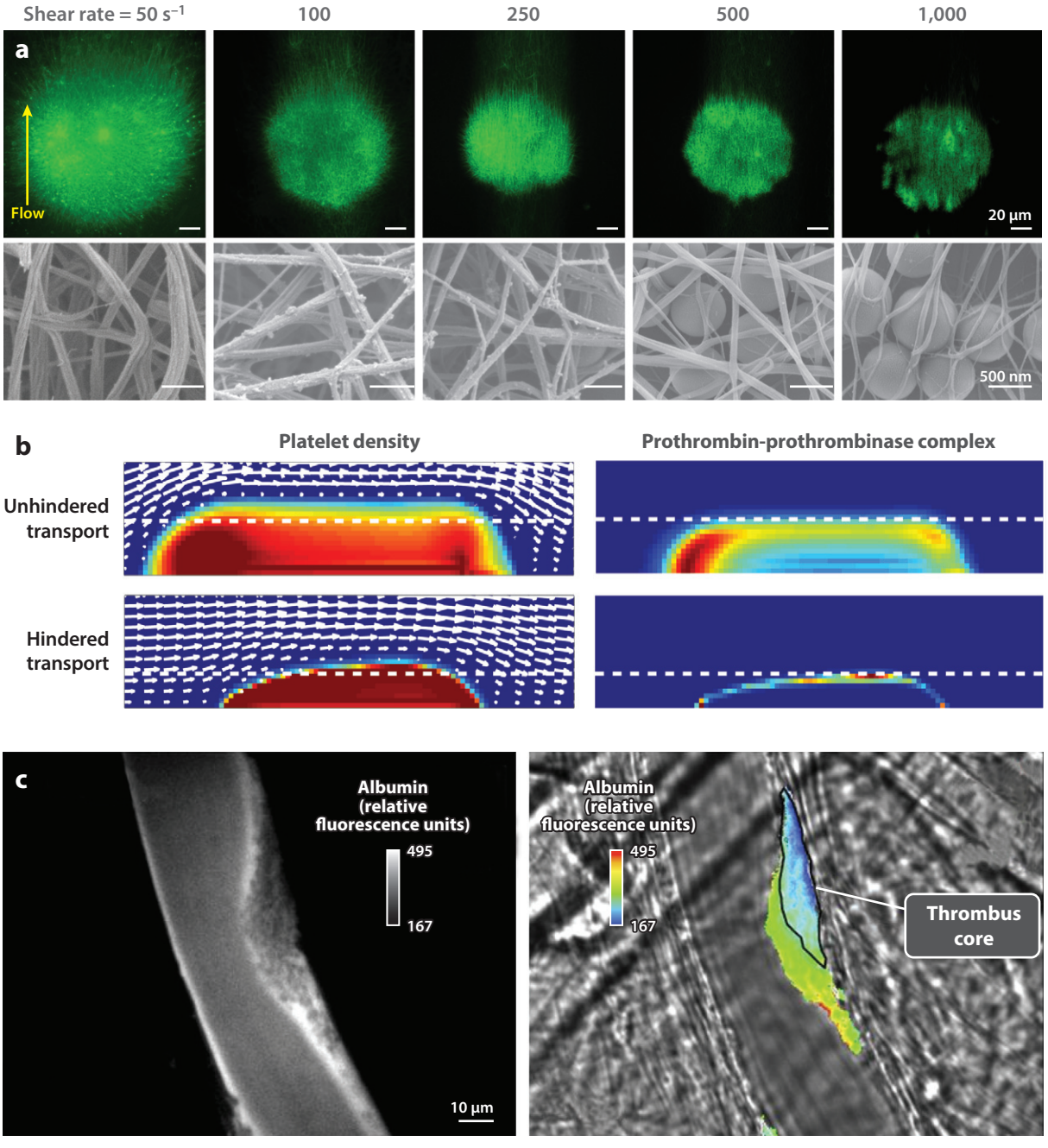

5.2. Physical Inhibition of Tissue Factor by Platelets

Most coagulation experiments are performed with purified protein solutions or plasma, ignoring the contribution of platelets to regulating coagulation. Platelets support coagulation by providing a surface for the assembly of tenase and prothrombinase, as well as binding sites for other coagulation proteins. Platelets inhibit coagulation by physically impeding access to TF:FVIIa. This mechanism was first hypothesized from simulations of hemophilia A and B (FVIII and FIX deficiency) that did not show a reduction in thrombin generation in the absence of some sort of physical inhibition of TF:FVIIa (Kuharsky & Fogelson 2001). It is supported by experiments under static conditions that show that FXa flux through a platelet plug is on the order of 10^3-fold less than FXa flux through fibrin (Hathcock & Nemerson 2004). Experiments performed under flow show that, at high TF concentrations, severe FVIII deficiencies (<1% normal levels) do not affect fibrin polymerization in plasma but lead to significant reductions in whole blood (Onasoga-Jarvis et al. 2013, 2014).

The tension between the platelets' pro- and anticoagulant roles underlies the TF threshold for initiating coagulation (Fogelson & Tania 2005) and the ability to make near-normal amounts of thrombin with 10% normal platelet concentrations in simulations (Kuharsky & Fogelson 2001). Experiments with blood perfused over the subendothelium at shear rates of 50–2,600 s^{-1} show that fibrin surface coverage and fibrinopeptide A generation (a marker for fibrin monomer production) decreased with increasing shear rate (Weiss et al. 1986). Fibrin deposition was independent of platelet adhesion below 100 s^{-1} but was positively correlated with platelet count in patients with low platelet counts (thrombocytopenia) at 650 s^{-1}. In contrast, fibrinopeptide A levels were not correlated to platelet count. This suggests that thrombin was being produced, but fibrin monomers and oligomers were not able to form fibers before being washed away by the flow.

5.3. Hindered Transport Through the Interstitial Spaces of Clots

Recent evidence suggests that, even beyond the role of SE-adherent platelets in blocking access to TF, the formation of platelet aggregates and fibrin gel inhibits solute transport in the clot, and this contributes to the regulation of clot growth. The clot takes on the character of a spatially heterogeneous porous medium, and fluid and solute transport through it are reduced compared to their transport to and from the vessel wall during clot initiation.

Computational models, in which transport coefficients decrease with increased bound platelet density, predict that hindered transport of coagulation zymogens and enzymes results in smaller,

Figure 5

Effects of transport. (*a*) Epifluorescent and scanning electron microscopy images of fibrin deposition on surface spots coated with tissue factor–bearing silica beads. The fibrin gel height and fiber thickness decrease with increasing shear rate. Fibers become progressively more aligned with the flow direction as the shear rate increases. Panel *a* reproduced with permission from Onasoga-Jarvis et al. (2014). (*b*) Simulations of thrombus growth in a model of platelet deposition and coagulation chemistry under flow. The thrombus is modeled as a porous medium with a permeability to the fluid flow decreasing as the density of bound platelets approaches the maximum packing density. For hindered transport simulations, the diffusion and advection of proteins were further hindered to reflect their macromolecular size. (*Left column*) Hindered protein transport produced smaller thrombi (*bottom*) with a uniformly highly dense core of platelets compared to the unhindered case. Colors indicate platelet count (number per unit volume) from normal plasma count (*dark blue*) to maximum platelet count within the thrombus (*dark red*). (*Right column*) Hindering protein transport severely limits the ability of fluid-phase prothrombin to penetrate the thrombus to reach platelet-bound prothrombinase (*bottom*) and so greatly reduces thrombin production. Colors indicate concentration from zero (*dark blue*) to maximum at the current time (*dark red*). Data for panel *b* obtained with the model described in Leiderman & Fogelson (2011, 2013). (*c*, *left*) Thrombus formation in the laser injury model in an arteriole of a mouse, showing the intensity of fluorescent albumin infused 25 min postinjury. Bright portions of the thrombus are more porous. (*Right*) Pseudocolor rendition of albumin fluorescent intensity in the thrombus. Relatively little albumin penetrates the thrombus core (*black outline*) consisting of tightly packed, strongly activated platelets. Panel *c* reproduced with permission from Stalker et al. (2013).

more dense clots (Leiderman & Fogelson 2013). Hindered transport confines activating complexes to a dense platelet core and reduces the supply of substrates to them. For example, in late stages of clot growth, the prothrombinase complex is concentrated on platelets near the vessel wall. For prothrombin to reach this prothrombinase, it must be transported through a shell of aggregated platelets that do not contain prothrombinase. As a result, prothrombin penetrates only deeply enough to reach prothrombinase in a thin strip several micrometers from the edge of the clot (**Figure 5*b***), and only there does thrombin production continue. Consequently, thrombin production decreases as the clot grows, limiting further clot growth.

These computational models agree qualitatively with the core-shell structure of clots formed in the laser-injury animal model of vascular injury (Stalker et al. 2013). The core consists of densely packed, highly activated platelets surrounded by a more porous shell of less activated platelets (**Figure 5*c***). Movement of solutes into and out of the core is limited (Welsh et al. 2012). Computational studies suggest another possible mechanism of hindered transport that involves a fibrin cap formed on the lumenal surface of a clot that prevents platelets from interacting with regions of high thrombin concentration in the clot core (Kim et al. 2013).

SUMMARY POINTS

1. Platelet margination is caused by platelet interactions with RBCs in flowing blood. Their motion in the RBC-rich vessel core scales similar to SID. An additional bias, or drift velocity, is necessary to eject platelets into the near-wall RBC depletion layer.
2. Platelet adhesion to the subendothelium at high shear stresses requires transient rolling mediated by weak, short-lived GPIb-vWF bonds followed by firm adhesion by strong, long-lived bonds mediated by activated integrins.
3. Platelet aggregation, or cohesion, at high shear stresses requires a two-step process initiated by GPIb-vWF bonds followed by activation by platelet-derived soluble agonists and firm attachment mediated by $\alpha_{IIb}\beta_3$.
4. vWF function and size are regulated by hydrodynamic forces in shear and extensional flows. Threshold forces are required to expose the domains responsible for its interactions with the platelet GPIb receptor and the enzyme ADAMTS-13 that regulates multimer size. This force threshold ensures that platelets only aggregate where shear forces are high (e.g., a vessel wall) and not while circulating.
5. Coagulation consists of two subprocesses: a tightly regulated network of biochemical reactions and the polymerization of the biopolymer fibrin. Under reaction-limited conditions, blood flow provides a continual source of reactants for these reactions. Under transport-limited conditions, blood flow dilutes coagulation products so that they do not accumulate near the injury site.
6. An above-threshold surface density of TF is necessary to initiate coagulation. The threshold ensures that the clotting process occurs only at injuries that are sufficiently large or deep.
7. Platelets serve a procoagulant role by supporting the assembly of coagulation enzyme complexes and serve an anticoagulation role by physically impeding access to TF.

8. Hindered solute transport in the interstitial spaces between platelets regulates clot growth by impeding access to immobilized coagulation enzyme complexes and limiting the escape of platelet agonists and coagulation products into the wider circulation.

DISCLOSURE STATEMENT

The authors are not aware of any biases that might be perceived as affecting the objectivity of this review.

ACKNOWLEDGMENTS

This work was supported in part by NSF grants DMS-1160432 and CBET-1351672, NIGMS grant 1R01GM090203-01, NHLBI grant R01HL120728, American Heart Association grant 14GRNT20410094, the Bayer Hemophilia Awards Program, and the Boettcher Foundation Webb-Waring Biomedical Research Awards.

LITERATURE CITED

Aarts PA, Steendijk P, Sixma JJ, Heethaar RM. 1986. Fluid shear as a possible mechanism for platelet diffusivity in flowing blood. *J. Biomech.* 19:799–805

Aarts PA, van den Broek SA, Prins GW, Kuiken GD, Sixma JJ, Heethaar RM. 1988. Blood platelets are concentrated near the wall and red blood cells, in the center in flowing blood. *Arteriosclerosis* 8:819–24

Alexander-Katz A, Netz RR. 2008. Dynamics and instabilities of collapsed polymers in shear flow. *Macromolecules* 41:3363–74

Alexander-Katz A, Schneider MF, Schneider SW, Wixforth A, Netz RR. 2006. Shear-flow-induced unfolding of polymeric globules. *Phys. Rev. Lett.* 97:138101

Andrews RK, Berndt MC. 2004. Platelet physiology and thrombosis. *Thromb. Res.* 114:447–53

Arya M, Anvari B, Romo GM, Cruz MA, Dong JF, et al. 2002a. Ultralarge multimers of von Willebrand factor form spontaneous high-strength bonds with the platelet glycoprotein Ib-IX complex: studies using optical tweezers. *Blood* 99:3971–77

Arya M, Lopez JA, Romo GM, Dong JF, McIntire LV, et al. 2002b. Measurement of the binding forces between von Willebrand factor and variants of platelet glycoprotein Ibα using optical tweezers. *Lasers Surg. Med.* 30:306–12

Broos K, Feys HB, De Meyer SF, Vanhoorelbeke K, Deckmyn H. 2011. Platelets at work in primary hemostasis. *Blood Rev.* 25:155–67

Charoenphol P, Huang RB, Eniola-Adefeso O. 2010. Potential role of size and hemodynamics in the efficacy of vascular-targeted spherical drug carriers. *Biomaterials* 31:1392–402

Chatterjee MS, Purvis JE, Brass LF, Diamond SL. 2010. Pairwise agonist scanning predicts cellular signaling responses to combinatorial stimuli. *Nat. Biotechnol.* 28:727–32

Chauhan AK, Motto DG, Lamb CB, Bergmeier W, Dockal M, et al. 2006. Systemic antithrombotic effects of ADAMTS13. *J. Exp. Med.* 208:767–76

Chen H, Angerer JI, Napoleone M, Reininger AJ, Schneider SW, et al. 2013. Hematocrit and flow rate regulate the adhesion of platelets to von Willebrand factor. *Biomicrofluidics* 7:064113

Chien S. 1987. Red cell deformability and its relevance to blood flow. *Annu. Rev. Physiol.* 49:177–92

Colace TV, Diamond SL. 2013. Direct observation of von Willebrand factor elongation and fiber formation on collagen during acute whole blood exposure to pathological flow. *Arterioscler. Thromb. Vasc. Biol.* 33:105–13

Colace TV, Muthard RW, Diamond SL. 2012. Thrombus growth and embolism on tissue factor-bearing collagen surfaces under flow: role of thrombin with and without fibrin. *Arterioscler. Thromb. Vasc. Biol.* 32:1466–76

Colman RW, Walsh PN. 1987. Mechanisms of platelet aggregation. In *Hemostasis and Thrombosis: Basic Principles and Clinical Practice*, ed. RW Colman, J Hirsh, VJ Marder, EW Salzman, pp. 594–605. Philadelphia: J.B. Lippincott

Crawley JTB, de Groot R, Xiang Y, Luken BM, Lane DA. 2011. von Willebrand factor unraveling the scissile bond: how ADAMTS-13 recognizes and cleaves. *Blood* 118:3212–21

Crowl L, Fogelson AL. 2011. Analysis of mechanisms for platelet near-wall excess under arterial blood flow conditions. *J. Fluid Mech.* 676:348–75

Dayananda KM, Singh I, Mondal N, Neelamegham S. 2010. von Willebrand factor self-association on platelet GPIbα under hydrodynamic shear: effect on shear-induced platelet activation. *Blood* 116:3990–98

De Ceunynck K, Rocha S, Feys HB, De Meyer SF, Uji-i H, et al. 2011. Local elongation of endothelial cell-anchored von Willebrand factor strings precedes ADAMTS13 protein-mediated proteolysis. *J. Biol. Chem.* 286:36361–67

Doggett TA, Girdhar G, Lawshe A, Schmidtke DW, Laurenzi IJ, et al. 2002. Selectin-like kinetics and biomechanics promote rapid platelet adhesion in flow: the GPIbα-vWF tether bond. *Biophys. J.* 83:184–205

Dong JF. 2005. Cleavage of ultra-large von Willebrand factor by ADAMTS-13 under flow conditions. *J. Thromb. Haemost.* 3:1710–16

Doshi N, Orje JN, Molins B, Smith JW, Mitragotri S, Ruggeri ZM. 2012. Platelet mimetic particles for targeting thrombi in flowing blood. *Adv. Mater.* 24:3864–69

Eckstein EC, Bailey DG, Shapiro AH. 1977. Self-diffusion of particles in shear flow of a suspension. *J. Fluid Mech.* 79:191–208

Eckstein EC, Belgacem F. 1991. Model of platelet transport in flowing blood with drift and diffusion terms. *Biophys. J.* 60:53–69

Eckstein EC, Tilles AW, Millero FJ III. 1988. Conditions for the occurrence of large near-wall excesses of small particles during blood flow. *Microvasc. Res.* 36:31–39

Filipovic N, Kojic M, Tsuda A. 2008. Modelling thrombosis using dissipative particle dynamics method. *Philos. Trans. R. Soc. A* 366:3265–79

Flamm MH, Colace T, Chatterjee M, Jing H, Zhou S, et al. 2012. Multiscale prediction of patient-specific platelet function under flow. *Blood* 120:190–98

Flamm MH, Diamond SL. 2012. Multiscale systems biology and physics of thrombosis under flow. *Ann. Biomed. Eng.* 40:2355–64

Flamm MH, Sinno T, Diamond SL. 2011. Simulation of aggregating particles in complex flows by the lattice kinetic Monte Carlo method. *J. Chem. Phys.* 134:034905

Fogelson AL. 1984. A mathematical model and numerical method for studying platelet adhesion and aggregation during blood clotting. *J. Comput. Phys.* 56:111–34

Fogelson AL. 1992. Continuum models of platelet aggregation: formulation and mechanical properties. *SIAM J. Appl. Math.* 52:1089–110

Fogelson AL. 1993. Continuum models of platelet aggregation: mechanical properties and chemically-induced phase transitions. *Contemp. Math.* 141:279–94

Fogelson AL, Guy RD. 2004. Platelet-wall interactions in continuum models of platelet aggregation: formulation and numerical solution. *Math. Med. Biol.* 21:293–334

Fogelson AL, Guy RD. 2008. Immersed-boundary-type models of intravascular platelet aggregation. *Comput. Methods Appl. Mech. Eng.* 197:2087–104

Fogelson AL, Kuharsky AL, Yu H. 2003. Computational modeling of blood clotting: coagulation and three-dimensional platelet aggregation. In *Polymer and Cell Dynamics: Multiscale Modeling and Numerical Simulations*, ed. W Alt, M Chaplain, M Griebel, J Lenz, pp. 145–54. Basel: Birkhäuser-Verlag

Fogelson AL, Tania N. 2005. Coagulation under flow: the influence of flow-mediated transport on the initiation and inhibition of coagulation. *Pathophysiol. Haemost. Thromb.* 34:91–108

Freund JB. 2013. Numerical simulation of flowing blood cells. *Annu. Rev. Fluid Mech.* 46:67–95

Furie B, Furie B. 2005. Thrombus formation in vivo. *J. Clin. Investig.* 115:3355–62

Galbusera M, Zoja C, Donadelli R, Paris S, Morigi M, et al. 1997. Fluid shear stress modulates von Willebrand factor release from human vascular endothelium. *Blood* 90:1558–64

Gemmell CH, Nemerson Y, Turitto V. 1990. The effects of shear rate on the enzymatic activity of the tissue factor-factor VIIa complex. *Microvasc. Res.* 40:327–40
Goldsmith HL. 1971. Red cell motions and wall interactions in tube flow. *Fed. Proc.* 30:1578–90
Goto S, Salomon DR, Ikeda Y, Ruggeri ZM. 1995. Characterization of the unique mechanism mediating the shear-dependent binding of soluble von Willebrand factor to platelets. *J. Biol. Chem.* 270:23352–61
Grabowski EF, Friedman LI, Leonard EF. 1972. Effects of shear rate on the diffusion and adhesion of blood platelets to a foreign surface. *Ind. Eng. Chem. Fundam.* 11:224–32
Guy RD, Fogelson AL, Keener JP. 2007. Modeling fibrin gel formation in a shear flow. *Math. Med. Biol.* 24:111–30
Hathcock J, Nemerson Y. 2004. Platelet deposition inhibits tissue factor activity: in vitro clots are impermeable to factor Xa. *Blood* 104:123–27
Haynes LM, Dubief YC, Orfeo T, Mann KG. 2011. Dilutional control of prothrombin activation at physiologically relevant shear rates. *Biophys. J.* 100:765–73
Hoffman M, Monroe DM. 2001. A cell-based model of hemostasis. *Thromb. Haemost.* 85:958–65
Jackson SP. 2007. The growing complexity of platelet aggregation. *Blood* 109:5087–95
Jackson SP, Nesbitt WS, Kulkarni S. 2003. Signaling events underlying thrombus formation. *J. Thromb. Haemost.* 1:1602–12
Jackson SP, Nesbitt WS, Westein E. 2009. Dynamics of platelet thrombus formation. *J. Thromb. Haemost.* 7:17–20
Jesty J, Nemerson Y. 1995. The pathways of blood coagulation. In *Williams Hematology*, ed. E Beutler, M Lichtman, B Coller, pp. 1227–38. New York: McGraw-Hill. 5th ed.
Jin SY, Skipwith CG, Shang D, Zheng XL. 2009. von Willebrand factor cleaved from endothelial cells by ADAMTS-13 remains ultralarge in size. *J. Thromb. Haemost.* 7:1749–52
Kamada H, Imai Y, Nakamura M, Ishikawa T, Yamaguchi T. 2013. Computational study on thrombus formation regulated by platelet glycoprotein and blood flow shear. *Microvasc. Res.* 89:95–106
Kamada H, Tsubota K, Nakamura M, Wada S, Ishikawa T, Yamaguchi T. 2010. A three-dimensional particle simulation of the formation and collapse of a primary thrombus. *Int. J. Numer. Methods Biomed. Eng.* 26:488–500
Kasirer-Friede A, Kahn ML, Shattil SJ. 2014. Platelet integrins and immunoreceptors. *Immunol. Rev.* 218:247–64
Kastrup C, Shen F, Runyon M, Ismagilov R. 2007. Characterization of the threshold response of initiation of blood clotting to stimulus patch size. *Biophys. J.* 93:2969–77
Kim J, Zhang CZ, Zhang X, Springer TA. 2010. A mechanically stabilized receptor-ligand flex-bond important in the vasculature. *Nature* 466:992–95
Kim OV, Xu Z, Rosen ED, Alber MS. 2013. Fibrin networks regulate protein transport during thrombus development. *PLoS Comput. Biol.* 9:e1003095
Kuharsky AL, Fogelson AL. 2001. Surface-mediated control of blood coagulation: the role of binding site densities and platelet deposition. *Biophys. J.* 80:1050–74
Kumar A, Graham MD. 2012. Mechanism of margination in confined flows of blood and other multicomponent suspensions. *Phys. Rev. Lett.* 109:108102
Leiderman K, Fogelson AL. 2011. Grow with the flow: a spatial-temporal model of platelet deposition and blood coagulation under flow. *Math. Med. Biol.* 28:47–84
Leiderman K, Fogelson AL. 2013. The influence of hindered transport on the development of platelet thrombi under flow. *Bull. Math. Biol.* 75:1255–83
Leighton D, Acrivos A. 1987. The shear-induced migration of particles in concentrated suspensions. *J. Fluid Mech.* 181:415–39
Li Z, Delaney MK, O'Brien KA, Du X. 2010. Signaling during platelet adhesion and activation. *Arterioscler. Thromb. Vasc. Biol.* 30:2341–49
Litvinov RI, Barsegov V, Schissler AJ, Fisher AR, Bennett JS, et al. 2011. Dissociation of bimolecular αIIbβ3-fibrinogen complex under a constant tensile force. *Biophys. J.* 100:165–73
Litvinov RI, Mekler A, Shuman H, Bennett JS, Barsegov V, Weisel JW. 2012. Resolving two-dimensional kinetics of the integrin αIIbβ3-fibrinogen interactions using binding-unbinding correlation spectroscopy. *J. Biol. Chem.* 287:35275–85

Mackman N. 2012. New insights into the mechanisms of venous thrombosis. *J. Clin. Investig.* 122:2331–36
Mann KG, Nesheim ME, Church WR, Haley P, Krishnaswamy S. 1990. Surface-dependent reactions of the vitamin K–dependent enzyme complexes. *Blood* 76:1–16
Matsui H, Sugimoto M, Mizuno T, Tsuji S, Miyata S, et al. 2002. Distinct and concerted functions of von Willebrand factor and fibrinogen in mural thrombus growth under high shear flow. *Blood* 100:3604–10
Maxwell MJ, Westein E, Nesbitt WS, Giuliano S, Dopheide SM, Jackson SP. 2007. Identification of a 2-stage platelet aggregation process mediating shear-dependent thrombus formation. *Blood* 109:566–76
Miura S, Li CQ, Cao H, Wang H, Wardell MR, Sadler JE. 2000. Interaction of von Willebrand factor domain A1 with platelet glycoprotein Ibα-(1–289). *J. Biol. Chem.* 275:7539–46
Mizuno T, Sugimoto M, Matsui H, Hamada M, Shida Y, Yoshioka A. 2008. Visual evaluation of blood coagulation during mural thrombogenesis under high shear blood flow. *Thromb. Res.* 121:855–64
Moake JL, Turner NA, Stathopoulos NA, Nolasco LH, Hellums JD. 1986. Involvement of large plasma von Willebrand factor (vWF) multimers and unusually large vWF forms derived from endothelial cells in shear stress-induced platelet aggregation. *J. Clin. Investig.* 78:1456–61
Moake JL, Turner NA, Stathopoulos NA, Nolasco LH, Hellums JD. 1988. Shear-induced platelet aggregation can be mediated by vWF released from platelets, as well as by exogenous large or unusually large vWF multimers, requires adenosine diphosphate, and is resistant to aspirin. *Blood* 71:1366–74
Mody NA, King MR. 2008a. Platelet adhesive dynamics. Part I: characterization of platelet hydrodynamic collisions and wall effects. *Biophys. J.* 95:2539–55
Mody NA, King MR. 2008b. Platelet adhesive dynamics. Part II: high shear-induced transient aggregation via GP1bα-vWF-GP1bα bridging. *Biophys. J.* 95:2556–74
Mori D, Yano K, Tsubota K, Ishikawa T, Wada S, Yamaguchi T. 2008. Simulation of platelet adhesion and aggregation regulated by fibrinogen and von Willebrand factor. *Thromb. Haemost.* 99:108–15
Narsimhan V, Zhao H, Shaqfeh ESG. 2013. Coarse-grained theory to predict the concentration distribution of red blood cells in wall-bounded Couette flow at zero Reynolds number. *Phys. Fluids* 25:061901
Neeves KB, Illing DAR, Diamond SL. 2010. Thrombin flux and wall shear rate regulate fibrin fiber deposition state during polymerization under flow. *Biophys. J.* 98:1344–52
Neeves KB, Onasoga AA, Hansen RR, Lilly JJ, Venckunaite D, et al. 2013. Sources of variability in platelet accumulation on type 1 fibrillar collagen in microfluidic flow assays. *PLoS ONE* 8:e54680
Okorie UM, Denney WS, Chatterjee MS, Neeves KB, Diamond SL. 2008. Determination of surface tissue factor thresholds that trigger coagulation at venous and arterial shear rates: Amplification of 100 fM circulating tissue factor requires flow. *Blood* 111:3507–13
Onasoga-Jarvis AA, Leiderman K, Fogelson AL, Wang M, Manco-Johnson MJ, et al. 2013. The effect of factor VIII deficiencies and replacement and bypass therapies on thrombus formation under venous flow conditions in microfluidic and computational models. *PLoS ONE* 8:e78732
Onasoga-Jarvis AA, Puls TJ, O'Brien SK, Kuang L, Liang HJ, Neeves KB. 2014. Thrombin generation and fibrin formation under flow on biomimetic tissue factor-rich surfaces. *J. Thromb. Haemost.* 12:373–82
Peterson DM, Stathopoulos NA, Giorgio TD, Hellums JD, Moake JL. 1987. Shear-induced platelet aggregation requires von Willebrand factor and platelet membrane glycoproteins Ib and IIb-IIIa. *Blood* 69:625–28
Phillips RJ, Armstrong RC, Brown RA, Graham AL, Abbott JR. 1992. A constitutive equation for concentrated suspensions that accounts for shear-induced particle migration. *Phys. Fluids* 4:30–40
Pivkin IV, Richardson PD, Karniadakis G. 2006. Blood flow velocity effects and role of activation delay time on growth and form of platelet thrombi. *Proc. Natl. Acad. Sci. USA* 103:17164–69
Pivkin IV, Richardson PD, Karniadakis G. 2009. Effect of red blood cells on platelet aggregation. *IEEE Eng. Med. Biol. Mag.* 28:32–37
Popel AS, Johnson PC. 2005. Microcirculation and hemorheology. *Annu. Rev. Fluid Mech.* 37:43–69
Pries AR, Neuhaus D, Gaehtgens P. 1992. Blood viscosity in tube flow: dependence on diameter and hematocrit. *Am. J. Physiol.* 263:H1770–78
Reasor DA, Mehrabadi M, Ku DN, Aidun CK. 2012. Determination of critical parameters in platelet margination. *Ann. Biomed. Eng.* 41:238–49

Repke D, Gemmell CH, Guha A, Turitto VT, Broze GJ, Nemerson Y. 1990. Hemophilia as a defect of the tissue factor pathway of blood coagulation: effect of factors VIII and IX on factor X activation in a continuous-flow reactor. *Proc. Natl. Acad. Sci. USA* 87:7623–27

Ruggeri ZM. 2009. Platelet adhesion under flow. *Microcirculation* 16:58–83

Ruggeri ZM, Dent JA, Saldivar E. 1999. Contribution of distinct adhesive interactions to platelet aggregation in flowing blood. *Blood* 94:172–78

Ruggeri ZM, Orje JN, Habermann R, Federici AB, Reininger AJ. 2006. Activation-independent platelet adhesion and aggregation under elevated shear stress. *Blood* 108:1903–10

Savage B, Almus-Jacobs F, Ruggeri ZM. 1998. Specific synergy of multiple substrate-receptor interactions in platelet thrombus formation under flow. *Cell* 94:657–66

Savage B, Saldivar E, Ruggeri ZM. 1996. Initiation of platelet adhesion by arrest onto fibrinogen or translocation on von Willebrand factor. *Cell* 84:289–97

Savage B, Sixma JJ, Ruggeri ZM. 2002. Functional self-association of von Willebrand factor during platelet adhesion under flow. *Proc. Natl. Acad. Sci. USA* 99:425–30

Schneider SW, Nuschele S, Wixforth A, Gorzelanny C, Alexander-Katz A, et al. 2007. Shear-induced unfolding triggers adhesion of von Willebrand factor fibers. *Proc. Natl. Acad. Sci. USA* 104:7899–903

Shankaran H, Alexandridis P, Neelamegham S. 2003. Aspects of hydrodynamic shear regulating shear-induced platelet activation and self-association of von Willebrand factor in suspension. *Blood* 101:2637–45

Shankaran H, Neelamegham S. 2004. Hydrodynamic forces applied on intercellular bonds, soluble molecules, and cell-surface receptors. *Biophys. J.* 86:576–88

Shen F, Kastrup CJ, Liu Y, Ismagilov RF. 2008. Threshold response of initiation of blood coagulation by tissue factor in patterned microfluidic capillaries is controlled by shear rate. *Arterioscler. Thromb. Vasc. Biol.* 28:2035–41

Shim K, Anderson PJ, Tuley EA, Wiswall E, Sadler EJ. 2008. Platelet-VWF complexes are preferred substrates of ADAMTS13 under fluid shear stress. *Blood* 111:651–57

Sing CE, Alexander-Katz A. 2010. Elongational flow induces unfolding of von Willebrand factor at physiological flow rates. *Biophys. J.* 98:L35–37

Sing CE, Alexander-Katz A. 2011. Dynamics of collapsed polymers under the simultaneous influence of elongational and shear flows. *J. Chem. Phys.* 135:014902

Skorczewski T, Erickson LC, Fogelson AL. 2013. Platelet motion near a vessel wall or thrombus surface in two-dimensional whole blood simulations. *Biophys. J.* 104:1764–72

Skorczewski T, Griffith BE, Fogelson AL. 2014. Multi-bond models for platelet adhesion and cohesion. *Contemp. Math.* In press

Smart JR, Leighton DT. 1991. Measurement of the drift of a droplet due to the presence of a plane. *Phys. Fluids A* 3:21–28

Spiel AO, Gilbert JC, Jilma B. 2008. von Willebrand factor in cardiovascular disease: focus on acute coronary syndromes. *Circulation* 117:1449–59

Stalker TJ, Traxler EA, Wu J, Wannemacher KM, Cermignano SL, et al. 2013. Hierarchical organization in the hemostatic response and its relationship to the platelet-signaling network. *Blood* 121:1875–85

Tangelder GJ, Slaaf DW, Teirlinck HC, Alewijnse R, Reneman RS. 1982. Localization within a thin optical section of fluorescent blood platelets flowing in a microvessel. *Microvasc. Res.* 23:214–30

Tangelder GJ, Teirlinck HC, Slaaf DW, Reneman RS. 1985. Distribution of blood platelets flowing in arterioles. *Am. J. Physiol.* 248:H318–23

Thomas WE, Vogel V, Sokurenko E. 2008. Biophysics of catch bonds. *Annu. Rev. Biophys.* 37:399–416

Thompson AJ, Mastria EM, Eniola-Adefeso O. 2013. The margination propensity of ellipsoidal micro/nanoparticles to the endothelium in human blood flow. *Biomaterials* 34:5863–71

Tilles AW, Eckstein EC. 1987. The near-wall excess of platelet-sized particles in blood flow: its dependence on hematocrit and wall shear rate. *Microvasc. Res.* 33:211–23

Tosenberger A, Ataullakhanov F, Bessonov N, Panteleev M, Tokarev A, Volpert V. 2013. Modelling of thrombus growth in flow with a DPD-PDE method. *J. Theor. Biol.* 337:30–41

Turitto VT, Baumgartner HR. 1975a. Platelet deposition on subendothelium exposed to flowing blood: mathematical analysis of physical parameters. *ASAIO J.* 21:593–601

Turitto VT, Baumgartner HR. 1975b. Platelet interaction with subendothelium in a perfusion system: physical role of red blood cells. *Microvasc. Res.* 9:335–44
Turitto VT, Benis AM, Leonard EF. 1972. Platelet diffusion in flowing blood. *Ind. Eng. Chem. Fundam.* 11:216–23
Turitto VT, Goldsmith HL. 1996. Rheology, transport and thrombosis in the circulation. In *Textbook of Vascular Medicine*, ed. J Loscalzo, M Creager, V Dzau, pp. 141–84. New York: Little, Brown. 2nd ed.
Turitto VT, Weiss HJ. 1980. Red blood cells: their dual role in thrombus formation. *Science* 207:541–43
Turner NA, Nolasco L, Moake JL. 2012. Generation and breakdown of soluble ultralarge von Willebrand factor multimers. *Semin. Thromb. Hemost.* 38:38–46
Turner NA, Nolasco L, Ruggeri ZM, Moake JL. 2009. Endothelial cell ADAMTS-13 and VWF: production, release, and VWF string cleavage. *Blood* 114:5102–11
Wang NT, Fogelson AL. 1999. Computational methods for continuum models of platelet aggregation. *J. Comput. Phys.* 151:649–75
Wang W, Diacovo TG, Chen J, Freund JB, King MR. 2013a. Simulation of platelet, thrombus and erythrocyte hydrodynamic interactions in a 3D arteriole with in vivo comparison. *PLoS ONE* 8:e76949
Wang W, King MR. 2012. Multiscale modeling of platelet adhesion and thrombus growth. *Ann. Biomed. Eng.* 40:2345–54
Wang W, Mody NA, King MR. 2013b. Multiscale model of platelet translocation and collision. *J. Comput. Phys.* 244:223–35
Watts T, Barigou M, Nash GB. 2013. Comparative rheology of the adhesion of platelets and leukocytes from flowing blood: Why are platelets so small? *Am. J. Physiol.* 304:H1483–94
Weisel JW. 2005. Fibrinogen and fibrin. *Adv. Protein Chem.* 70:247–99
Weiss HJ, Turitto VT, Baumgartner HR. 1986. Role of shear rate and platelets in promoting fibrin formation on rabbit subendothelium: studies utilizing patients with quantitative and qualitative platelet defects. *J. Clin. Investig.* 78:1072–82
Welsh JD, Colace TV, Muthard RW, Stalker TJ, Brass LF, Diamond SL. 2012. Platelet-targeting sensor reveals thrombin gradients within blood clots forming in microfluidic assays and in mouse. *J. Thromb. Haemost.* 10:2344–53
Westein E, van der Meerc A, Kuijpers MJE, Frimat JP, van den Berg A, Heemskerk JWM. 2013. Atherosclerotic geometries exacerbate pathological thrombus formation poststenosis in a von Willebrand factor-dependent manner. *Proc. Natl. Acad. Sci. USA* 110:1357–62
Woldhuis B, Tangelder GJ, Slaaf DW, Reneman RS. 1992. Concentration profile of blood platelets differs in arterioles and venules. *Am. J. Physiol.* 262:H1217–23
Wu T, Lin J, Cruz MA, Dong JF, Zhu C. 2010. Force-induced cleavage of single VWFA1A2A3 tridomains by ADAMTS-13. *Blood* 115:370–78
Wufsus AR, Macera NE, Neeves KB. 2013. The hydraulic permeability of blood clots as a function of fibrin and platelet density. *Biophys. J.* 104:1812–23
Xu C, Wootton D. 2004. Platelet near-wall excess in porcine whole blood in artery-sized tubes under steady and pulsatile flow conditions. *Biorheology* 41:113–25
Xu Z, Chen N, Kamocka MM, Rosen ED, Alber M. 2008. A multiscale model of thrombus development. *J. R. Soc. Interface* 5:705–22
Xu Z, Chen N, Shadden SC, Marsden JE, Kamocka MM, et al. 2009. Study of blood flow impact on growth of thrombi using a multiscale model. *Soft Matter* 5:769–79
Xu Z, Kamocka MM, Alber M, Rosen ED. 2011. Computational approaches to studying thrombus development. *Ateriosclerosis. Thromb. Vasc. Biol.* 31:500–5
Xu Z, Lioi J, Mu J, Kamocka MM, Liu X, et al. 2010. A multiscale model of venous thrombus formation with surface-mediated control of blood coagulation cascade. *Biophys. J.* 98:1723–32
Yago T, Lou J, Wu T, Yang J, Miner J, et al. 2008. Platelet glycoprotein Ibα forms catch bonds with human WT vWF but not with type 2B von Willebrand disease vWF. *J. Clin. Investig.* 118:3195–207
Yeh C, Calvez AC, Eckstein EC. 1994. An estimated shape function for drift in a platelet-transport model. *Biophys. J.* 67:1252–59
Ying J, Ling Y, Westfield L, Sadler J, Shao JY. 2010. Unfolding the A2 domain of von Willebrand factor with the optical trap. *Biophys. J.* 98:1685–93

Zhang X, Halvorsen K, Zhang CZ, Wong WP, Springer TA. 2009. Mechanoenzymatic cleavage of the ultralarge vascular protein von Willebrand factor. *Science* 324:1330–34

Zhao H, Shaqfeh ESG, Narsimhan V. 2012. Shear-induced particle migration and margination in a cellular suspension. *Phys. Fluids* 24:011902

Zhao R, Kameneva M, Antaki J. 2007. Investigation of platelet margination phenomena at elevated shear stress. *Biorheology* 44:161–77

Zhou Z, Nguyen TC, Guchhait P, Dong JF. 2010. Von Willebrand factor, ADAMTS-13, and thrombotic thrombocytopenic purpura. *Semin. Thromb. Hemost.* 36:71–81

Zydney AL, Colton CK. 1988. Augmented solute transport in the shear flow of a concentrated suspension. *Physicochem. Hydrodyn.* 10:77–96

Annual Review of
Fluid Mechanics

Volume 47, 2015

Contents

Indexes

Errata

An online log of corrections to *Annual Review of Fluid Mechanics* articles may be found at http://www.annualreviews.org/errata/fluid